Article

Morpho-Molecular Discordance? Re-Approaching Systematics of *Cambeva* (Siluriformes: Trichomycteridae) from the Guaratuba-Babitonga-Itapocu Area, Southern Brazil

Wilson J. E. M. Costa [1,*] , **Caio R. M. Feltrin** [1] , **José Leonardo O. Mattos** [1] , **Roger H. Dalcin** [2] , **Vinicius Abilhoa** [3] **and Axel M. Katz** [1]

1   Laboratory of Systematics and Evolution of Teleost Fishes, Institute of Biology, Federal University of Rio de Janeiro, Rio de Janeiro 21941-971, Brazil
2   Programa de Pós-Graduação em Zoologia, Universidade Federal do Paraná, Curitiba 81531-980, Brazil
3   Museu de História Natural Capão da Imbuia, Curitiba 82810-080, Brazil
*   Correspondence: wcosta@acd.ufrj.br

Abstract: A recent field inventory focusing on catfishes of the trichomycterine genus *Cambeva* detected the occurrence of two morphotypes, *C. barbosae* and *C. cubataonis*, in the Guaratuba-Babitonga-Itapocu area (GBIA) of southern Brazil, reporting some discordance with results of coalescent-based approaches for species delimitation that indicated different estimates of species number. Contrastingly, based on examination of characters taken from the external morphology and osteology, we here recognised six species of *Cambeva* in GBIA: *C.* cf. *botuvera*, a polymorphic and geographically widespread species; *C. cubataonis*, endemic to the Rio Cubatão do Norte; and four new species, two endemic to the Rio Itapocu basin, one endemic to the Baía de Babitonga system and one endemic to the Baía de Guaratuba system. We performed a molecular phylogenetic analysis indicating that *Cambeva* comprises three major clades, the alpha-, beta- and gama-clades, with *C.* cf. *botuvera* and a clade comprising *C. cubataonis* and three new species belonging to the beta-clade and another new species belonging to the gama-clade. We concluded that species here recognised are not in fact incongruent with results of that recent study when taxa are correctly identified by a representative sample of morphological characters, highlighting the importance of osteological characters for delimiting trichomycterine species.

Keywords: Atlantic Forest; comparative osteology; mountain biodiversity; molecular phylogeny; new species

1. Introduction

The Neotropical Region harbours the most diverse freshwater fish fauna on earth, with more than 6200 species distributed throughout the continental waters from Mexico to the southernmost tip of South America [1]. Despite recent efforts directed to describe the Neotropical ichthyofauna, several components are still little known, with many species still waiting for formal descriptions. Among them is the Trichomycterinae, a subfamily of Trichomycteridae catfishes, presently represented by 282 species found in fast-flowing streams of South America and southern Central America [2]. About half of these species belongs to a clade endemic to eastern South America that includes the genera *Cambeva* Katz, Barbosa, Mattos & Costa, 2018, *Scleronema* Eigenmann, 1917 and *Trichomycterus s.s.* Valenciennes, 1832, called the CST-clade [3]. In the last three years, 39 new trichomycterine species of phylogenetic lineages little or not previously known were described from eastern and central South American region [4–20], demonstrating that our current knowledge about this group is still at an initial stage. *Cambeva*, the focus of the present study, includes over 40 species [9], many of them with restricted distribution, occurring between the Rio

São Francisco basin in south-eastern Brazil and tributaries of the Lagoa dos Patos system in southern Brazil [21].

One of the most sampled areas in our recent field studies comprises the Rio Itapocu and the adjacent drainages that flow into the Baía de Babitonga and in the Baía de Guaratuba (hereafter the Guaratuba-Babitonga-Itapocu area, GBIA), corresponding to the north-eastern portion of Santa Catarina State, in southern Brazil. As in other regions located on the east side of the Serra do Mar, the coastal rivers rise with typical characteristics of mountain rivers and change to more slowly flowing when they reach the coastal plain [22]. Only *Cambeva cubataonis* (Bizerril, 1994) was formally described for GBIA [23], which is part of the Atlantic Forest, one of the most threatened and richest biomes on earth [24–27]. In GBIA, most original forests located on the coastal plain were extirpated to make way for plantations, industries and urban centres [28]. Consequently, some rivers located in the GBIA have high levels of physical degradation and pollution, making fish species vulnerable or even highly endangered [29]. In our field studies in GBIA, in addition to *C. cubataonis*, we were able to recognise four species not yet described and a widely distributed one with a high level of chromatic polymorphism, identified as *Cambeva* cf. *botuvera* Costa, Feltrin & Katz, 2021.

In a recent paper, Donin et al. [30] provided an estimate on species limits in populations of *Cambeva* from the coastal basins of south-eastern and southern Brazil, integrating morphological data and coalescent-based approaches using a short segment (597 bp) of the mitochondrial gene *cytochrome oxidase c subunit 1* (COX1). Among populations found in GBIA, only *C. barbosae* Costa, Feltrin & Katz, 2021 and *C. cubataonis* were recognised by them. In the phylogenetic tree included in the text [30] (Figure 11 in Ref. [30]), *C. barbosae* and *C. cubataonis* clustered together at the same molecularly delimited entity, thus indicating to be a single species, whereas morphotypes also identified as *C. cubataonis* appeared as three distinct delimited species of another intrageneric subclade. The occurrence of the same morphotype in different molecularly delimited species belonging to different intrageneric subclades was interpreted by Donin et al. [30] as a possible result of mitochondrial introgression and incomplete lineage sorting, concluding that single-locus data were insufficient to delimit species of *Cambeva*, which would implicate in some discordance between morphological and molecular data.

In the present study, we list *Cambeva* species found in our field inventories in GBIA, providing formal descriptions for four new species, using morphological diagnosability criterion to delimit them. Since our field studies indicated that some species of *Cambeva* occurring in GBIA are rare and high levels of habitat disturbance were recorded, we also provide habitat notes for each species. Next, we perform a molecular phylogenetic analysis, consisting in the most comprehensive taxon sample for *Cambeva*, to infer the phylogenetic position of species from GBIA among the major lineages of the genus. Finally, we compare our results with results of Donin et al. [30] for species from GBIA, in order to check if molecular data are incongruent or not with morphological variation.

2. Materials and Methods

2.1. Specimens

Specimens were collected using dip nets, with collecting permits given by ICMBio (Instituto Chico Mendes de Conservação da Biodiversidade; permit numbers: 38553-13 and 10320-1). Euthanasia followed the AVMA Guidelines for the Euthanasia of Animals [31], using a buffered solution of tricaine methane sulphonate (MS-222) at a concentration of 250 mg/L, or eugenol solution, in accordance to the methods approved by CEUA-CCS-UFRJ (Ethics Committee for Animal Use of Federal University of Rio de Janeiro; permit number: 065/18). Specimens used in morphological studies were fixed in formalin for two weeks, and then transferred to 70% ethanol. Specimens cleared and stained for osteological analyses according to Taylor & Van Dyke [32] were preserved in glycerine; the abbreviation C&S indicates cleared and stained specimens in lists of the material examined. Specimens used in molecular analysis were fixed and preserved in absolute ethanol; in lists of material

examined, the abbreviation DNA indicates these specimens. Most material used in this study was deposited in the Instituto de Biologia, Universidade Federal do Rio de Janeiro (UFRJ); some specimens were deposited in the Centro de Ciências Agrárias e Ambientais, Universidade Federal do Maranhão (CICCAA) and Museu de História Natural Capão da Imbuia (MHNCI), Curitiba. In lists of examined material specimens, geographical names correspond to Portuguese names used in the region. Comparative material appears in Costa et al. [4,6,7,9–11].

2.2. Morphological Data

Measurements were made using landmarks described by Costa [33] and modified by Costa et al. [34]. Measurements are expressed as percent of standard length (SL) or head length. Only well-preserved specimens above 40 mm SL were measured. Fin-ray formulae followed Costa et al. [34], which follows standards described in Bockmann & Sazima [35]. Vertebra counts include all elements, except the Apparatus of Weber. Osteological illustrations were first made in a stereomicroscope Zeiss Stemi SV 6 with camera lucida. Terminology for osteological structures is according to Costa [3] and for pores of the latero-sensory system, to Arratia and Huaquin [36], with modifications proposed by Bockmann & Sazima [35].

Comparative morphological analyses, including characters taken from the external morphology and osteology, were performed to search for character states useful to diagnose new species from GBIA. Species were then delimited using a diagnosability criterion [37], in which species are recognised through unique combinations of stable morphological character states occurring in one or more populations as described by Davis & Nixon [38].

2.3. DNA Extraction, Amplification and Sequencing

The genomic DNA of specimens was extracted from the caudal peduncle muscle tissue using DNeasy Blood & Tissue Kit (Qiagen, Venlo, The Netherlands). DNA extract quality was visually evaluated by agarose gel electrophoresis. The polymerase chain reaction (PCR) method was followed to amplify the target DNA fragments, using the following DNA oligos: Cytb Siluri F and Cytb Siluri R [39], CatThr29 and Glu 31 [40], and Glu 5 and Cb23 [41] for the mitochondrial gene *cytochrome b* (CYTB); FISHF1 and FISHR1 [42] for the mitochondrial gene *cytochrome c oxidase I* (COX1); MHRAG2-F1 and MHRAG2-R1 [43], RAG2 TRICHO F and RAG2 TRICHO R [44], and RAG2 MCF and RAG2 MCR [45] for the nuclear gene *recombination activating 2* (RAG2). The PCR reactions were performed in 50 μL with the following reagent concentrations: 5× GreenGoTaq Reaction Buffer (Promega, Madison, WI, USA), 2.0 mM $MgCl_2$, 1 μM of each primer, 0.2 mM of each dNTP, 1 u of Promega GoTaq Hot Start polymerase and 50 ng of total genomic DNA. Negative controls were used to check for contaminants in all reactions. The thermocycling profile was: initial denaturation for 2–5 min at 9495 °C; 35 cycles of denaturation for 1 min at 94–95 °C, annealing for 0.5–1 min at 45–55 °C and extension for 1–1.2 min at 72 °C; and final extension for 7 min at 72 °C. The PCR products were purified using the Wizard SV Gel and PCR Clean-Up System (Promega). Sequencing reactions were made using the BigDye Terminator Cycle Sequencing Mix (Applied Biosystems, Waltham, MA, USA). Cycle sequencing reactions were performed in 20 μL reaction volumes containing 4 μL BigDye, 2 μL sequencing buffer 5× (Applied Biosystems), 2 μL of the amplified products (20–40 ng), 2 μL primer and 10 μL deionised water. The thermocycling profile was 35 cycles of 10 s at 96 °C, 5 s at 54 °C and 4 min at 60 °C. Interpretation of chromatograms and edition of the sequences were performed using MEGA 11 [46]. The DNA sequences were translated into amino acid residues using the program MEGA 11 to verify the correct codification of each sequence, and the absence of premature stop codons or indels. GenBank accession numbers are provided in Appendix A.

2.4. Phylogenetic Analysis

Terminal taxa comprised the six species of *Cambeva* occurring in GBIA and other 24 congeners representing all intrageneric lineages. Outgroups were two species of *Scleronema*, the sister group of *Cambeva*; two species of *Trichomycterus s.s.*, the sister group of *Cambeva* plus *Scleronema*; three trichomycterine species representing other subfamilial lineages; four species representing other trichomycterid subfamilies; and one nematogenyid species, the sister group of the Trichomycteridae. The analysis comprises both DNA sequences here generated and those taken from GenBank and first published in Ochoa et al. [47], Katz et al. [21] and Donin et al. [30]. Gene data sets were separately aligned using the Clustal W algorithm [48] in MEGA 11. No stop codons and gaps were found. The concatenated molecular data matrix had 2303 bp (COX1 522 bp, CYTB 993 bp, RAG2 788 bp). The PartitionFinder2.1.1 [49] algorithm was used to obtain the best-fit partitions and evolutive model schemes (provided in Appendix B), under the Corrected Akaike Information Criterion (AICc). Two independent phylogenetic reconstruction methods were employed in the phylogenetic analyses, Bayesian Inference (BI) and Maximum Likelihood (ML) analyses. BI was conducted using Mrbayes 3.2.5 [50], applying two independent Markov chain Monte Carlo (MCMC) runs of two chains each for 5×10^6 generations, with a sampling frequency of every 1000 generations. The convergence of the MCMC chains and the proper burn-in value were established with Tracer 1.7.1 [51]. The consensus tree and Bayesian posterior probabilities were calculated after removing the first 25% samples. ML was conducted using IQTREE 2.2.0 [52], and the support of the nodes were evaluated by calculation of 1000 ultrafast bootstrap [53], and 1000 bootstrap [54] replicates.

3. Results

3.1. Phylogenetic Relationships of Cambeva Species from GBIA

Although the phylogenetic analysis here performed contains the best sampling of terminal taxa of *Cambeva*, it is far from representing the entire genus. Even so, clades endemic to certain regions are well supported in the analysis, sometimes corroborating morphological studies as below described. The phylogenetic analysis supported three major clades in *Cambeva* (Figure 1). The first clade, here named as the *Cambeva* alpha-clade, is sister to a clade comprising all other congeners. This clade comprises species occurring in the northern part of the genus distribution, including the Rio São Francisco basin and the upper Rio Paraná basin, but overlapped in its southern portion with the distribution of the *Cambeva* beta-clade (see below) in the smaller river basins of south-eastern Brazil (Figure 2). Species of the *Cambeva* alpha-clade are distinguished from other congeners by having ten or eleven principal dorsal-fin rays (vs. always nine). This clade corresponds to the clade C in the genealogical COX1 tree of Donin et al. [30] (Figure 11 in Ref. [30]). No species of the *Cambeva* alpha-clade were found in GBIA.

The two other main clades, the *Cambeva* beta- and gama-clades, nearly correspond to groups proposed by Costa et al. [6] but cannot be presently diagnosed by unique morphological character states. According to the phylogenetic analysis, *Cambeva naipi* (Wosiacki & Garavello, 2004) is sister to a clade comprising the beta- and gama-clades, therefore not included in any of them. The *Cambeva* beta-clade, similar to the *C. davisi* group of Costa et al. [6] and clade B of Donin et al. [30], occupies the central portion of the genus distribution, including the upper Rio Paraná basin and adjacent coastal basins (Figure 2). Four species from GBIA, *C.* cf. *botuvera*, *C. cubataonis* and three undescribed species (*Cambeva chrysornata* sp. nov., *Cambeva guaratuba* sp. nov., and *Cambeva ventropapillata* sp. nov.), belong to the *Cambeva* beta-clade.

The geographically widespread *C.* cf. *botuvera*, found in all areas of GBIA (Figure 3), was supported as sister to *C. botuvera*, and both are contained in a well-supported clade also including *C. barbosae*, *Cambeva castroi* (de Pinna, 1992), *Cambeva davisi* (Haseman, 1911), *Cambeva* cf. *diabola* (Bockmann, Casatti & de Pinna, 2004) and *Cambeva stawiarski* (Miranda Ribeiro, 1968). *Cambeva cubataonis* and three new species from GBIA were supported as monophyletic, with high support values. A new species from the Rio Itapocu basin (*C.*

ventropapillata sp. nov.; Figure 4) appeared as sister to a clade comprising *C. cubataonis* and two undescribed species (*C. chrysornata* sp. nov. and *C. guaratuba* sp. nov.). However, morphological characters highly suggest that this new species from the Rio Itapocu basin is more closely related to *Cambeva papillifera* (Wosiacki & Garavello, 2004), not available for the molecular analysis, by both sharing some unique morphological features, including the presence of a broad laminar, ribbon-shaped nasal barbel; maxillary and rictal barbels broad at their basal portion, abruptly narrowing distally; and large skin papillae on the ventral surface of the head (see diagnosis and description of the new species below). The clade here supported comprising *C. cubataonis* and two undescribed species is morphologically supported by adult specimens, above about 40 mm SL, having a unique colour pattern, in which the flank and the dorsum are predominantly dark grey to black contrasting with bright yellow marks (vs. never a similar colour pattern) and having odontodes with a rounded extremity at least on the internal-most series of the interopercle (vs. pointed odontodes). A new species from the Rio São João basin, Baía de Guaratuba system (*C. guaratuba* sp. nov.), is supported as sister to a clade comprising *C. cubataonis*, endemic to the Rio Cubatão do Norte basin that is associated to the Baía de Babitonga system, and a new species from the Rio Palmital basin (*C. chrysornata* sp. nov.), which is also associated with the Baía de Babitonga system (Figure 4). Species of the last clade share a peculiar morphology of the autopalatine, as below described and illustrated in Taxonomical Accounts.
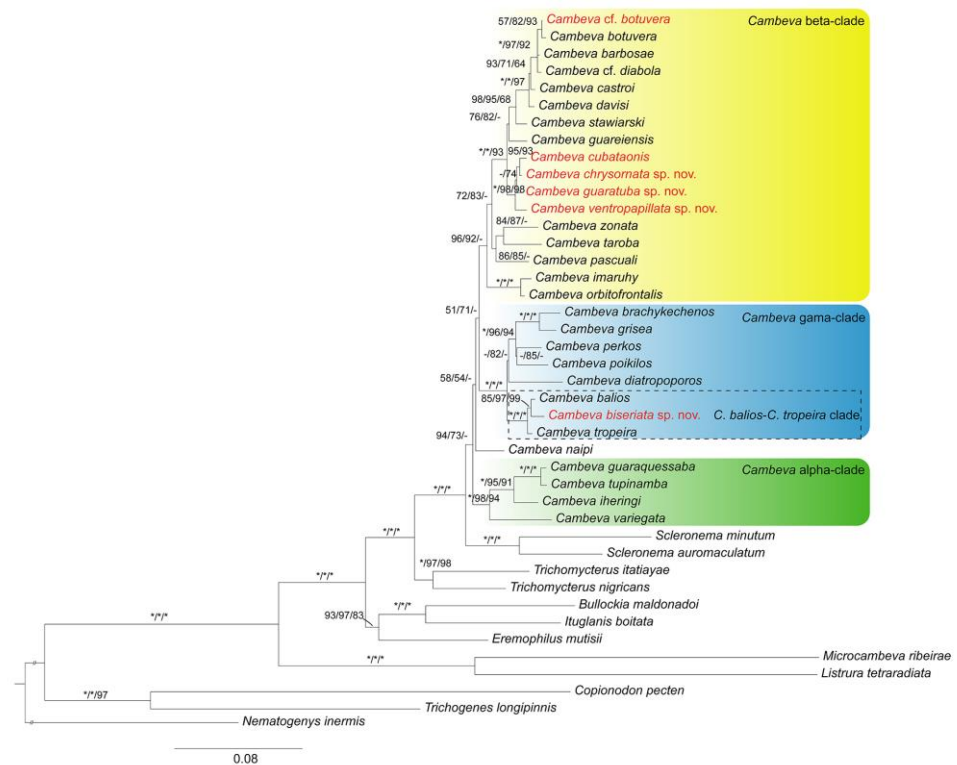

Figure 1. Maximum likelihood tree estimated by IQ-tree for 30 species of *Cambeva* and 12 outgroups, combining three genes (COI, CYTB, and RAG2), total of 2303 bp). The numbers above branches indicate Bayesian posterior probabilities of the Bayesian inference analysis, bootstrap and fast bootstrap values of the maximum likelihood analyses, respectively, separated by a bar. Asterisks (*) indicate maximum support values and dashes (-) indicate values below 50. Taxa in red are species from the Guaratuba-Babitonga-Itapocu area.
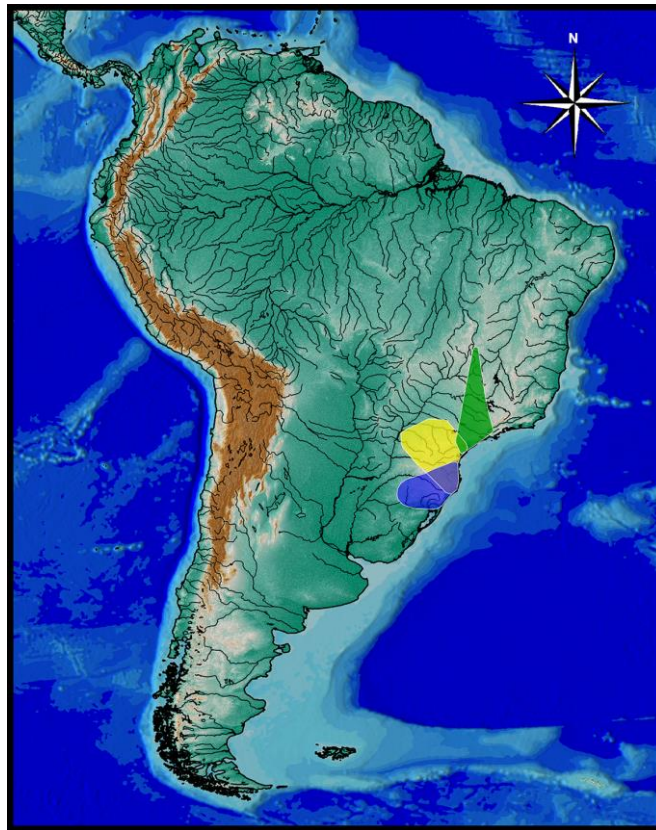
Figure 2. Geographical distribution of the three main clades of *Cambeva*. Green—alpha-clade; yellow—beta-clade; blue—gama-clade.
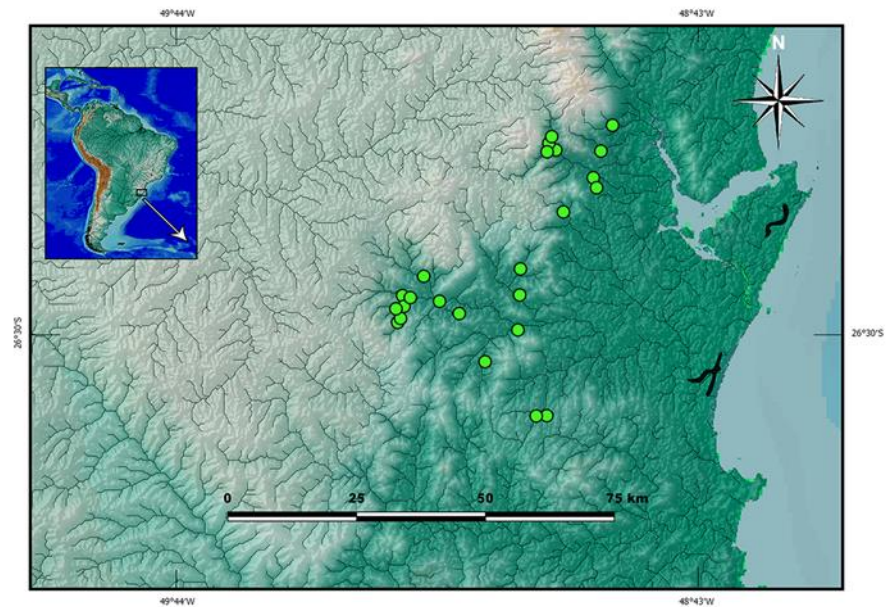

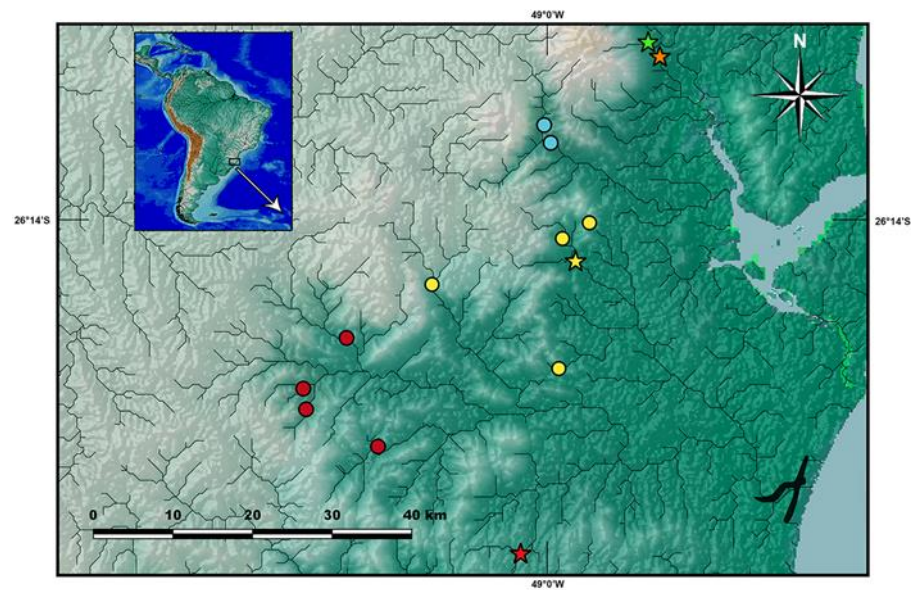**Figure 3.** Geographical distribution of *Cambeva* cf. *botuvera*.

Figure 4. Geographical distribution of *Cambeva biseriata* sp. nov. (yellow), *Cambeva chrysornata* sp. nov. (orange), *Cambeva cubataonis* (blue) and *Cambeva ventropapillata* sp. nov. (red). Stars indicate type localities.

The *Cambeva* gama-clade mostly includes species occurring in the southern portion of the genus distribution, including river basins connected with the Lagoa dos Patos system and the Rio Uruguai basin, but also includes species with their distribution overlapping the distribution of species of the *Cambeva* beta-clade in the coastal basins of southern Brazil (Figure 2). The *Cambeva* gama-clade is similar to the *C. balios* group delimited by Costa et al. [6] and the clade A of Donin et al. [30]. The only species of this clade occurring in GBIA is a new species from the Rio Itapocu basin (*Cambeva biseriata* sp. nov.), which is supported to be a member of a clade including *C. balios* (Ferrer & Malabarba, 2013) and *C. tropeira* (Ferrer & Malabarba, 2011). This clade here named as the *C. balios*-*C. tropeira* clade may be diagnosed by a combination of morphological features including the presence of dark grey to black spots over a lighter ground on the flank (vs. never a similar colour pattern), seven pectoral-fin rays (vs. five, six or eight), three or four procurrent rays on the dorsal and anal fins (vs. two), relatively few interopercular odontodes (15–25, vs. 26–36), and a lateral process on the sesamoid supraorbital (vs. absence). Species of the *C. balios*-*C. tropeira* clade may be also distinguished from other species of the *Cambeva* gama-clade by having a relatively narrow autopalatine with a well-developed postero-lateral process, contrasting with the broad autopalatine with short or rudimentary postero-lateral process [4].

According to Costa et al. [7], species of the *C. balios*-*C. tropeira* clade may be grouped in two assemblages, the *C. balios* complex, with species reaching a large size (at least about 100 mm of standard length, SL) and always lacking the anterior section of the infraorbital canal, comprising *C. balios*, *Cambeva diffusa* Costa, Feltrin & Katz, 2021, and *Cambeva pericoh* Costa, Feltrin & Katz, 2021; and the *C. tropeira* complex, with species reaching a smaller size (about 85 mm SL or less) and having a well-developed anterior section of the infraorbital canal, comprising *C. duplimaculata* Costa, Feltrin & Katz, 2021, *C. longipalata* Costa, Feltrin & Katz, 2021, *C. notabilis* Costa, Feltrin & Katz, 2021, *C. tropeira*, and *C. urubici* Costa, Feltrin & Katz, 2021. The phylogenetic analysis, including only *C. balios*, *C. tropeira* and the new species, supported the new species as being closely related to *C. balios* than to *C. tropeira*, which is congruent with the absence of the anterior section of the infraorbital series shared by the new species and species of the *C. balios* complex. However, the maximum recorded size of the new species is only about 75 mm SL. The presence of a long postero-lateral process of the autopalatine, its length about equal to the autopalatine length excluding that

process, occurring only in the new species (see description below) and *C. longipalata* [7] (Figure 11H in Ref. [7]), may be an indicative of close relationships.

3.2. Taxonomic Accounts

3.2.1. *Cambeva* Beta-Clade

Cambeva cf. *Cambeva botuvera* Costa, Feltrin & Katz, 2021

Trichomycterus cubataonis (non *Trichomycterus cubataonis* Bizerril, 1994): Katz & Barbosa [55] (pp. 4–6, Figures 2 and 3 in Ref. [55]) (misidentification).

Figures 5, 6, 7A, 8A and 9A, respectively.

Remarks. The taxon here identified as *C.* cf. *botuvera* is broadly distributed in GBIA (Figure 3). It is still unclear whether it represents a morphologically polymorphic species or a species complex. Some colour morphs are not distinguishable from some colour morphs described for *C. barbosae* and *C. botuvera* [6] (p. 5, Figure 3 in Ref. [6]), whereas different populations from GBIA may exhibit distinct morphological traits. On the other hand, our molecular studies in progress indicate low genetic differentiation among GBIA populations. Like *C. botuvera*, *C.* cf. *botuvera* has eight rays in the pectoral fin, instead of seven as in *C. barbosae*. This complex group is presently the focus of a specific study on species delimitation that is in progress by the authors, encompassing a broader geographical area much beyond the limits of GBIA.

Figure 5. *Cambeva* cf. *botuvera*, UFRJ 13269, Rio Cubatão do Norte basin, spotted morph, 60.8 mm SL: (**A**) lateral, (**B**) dorsal, and (**C**) ventral views.
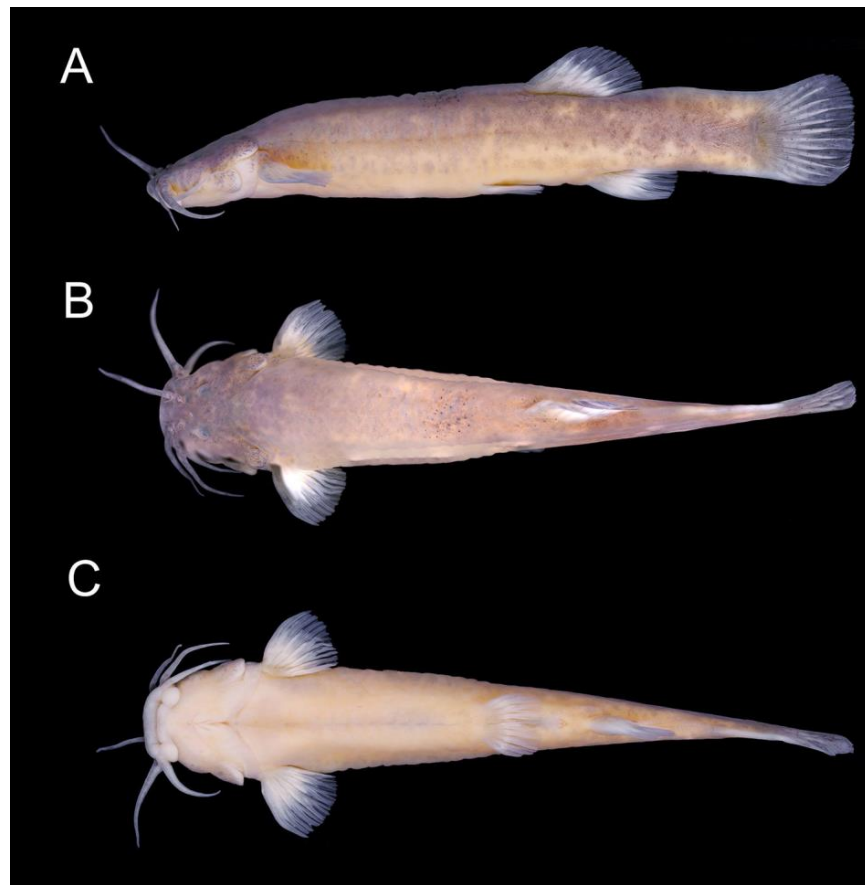
Figure 6. *Cambeva* cf. *botuvera*, UFRJ 13269, Rio Cubatão do Norte basin, dark-coloured morph, 65.2 mm SL: (**A**) lateral, (**B**) dorsal, and (**C**) ventral views.

Figure 7. Mesethmoidal region, middle and left portions, dorsal view: (**A**) *Cambeva* cf. *botuvera*; (**B**) *Cambeva chrysornata* sp. nov.; (**C**) *Cambeva cubataonis*; (**D**) *Cambeva guaratuba* sp. nov.; (**E**) *Cambeva ventropapillata* sp. nov.; (**F**) *Cambeva biseriata* sp. nov. Larger stippling represents cartilage. Arrow indicates the autopalatine medial expansion.

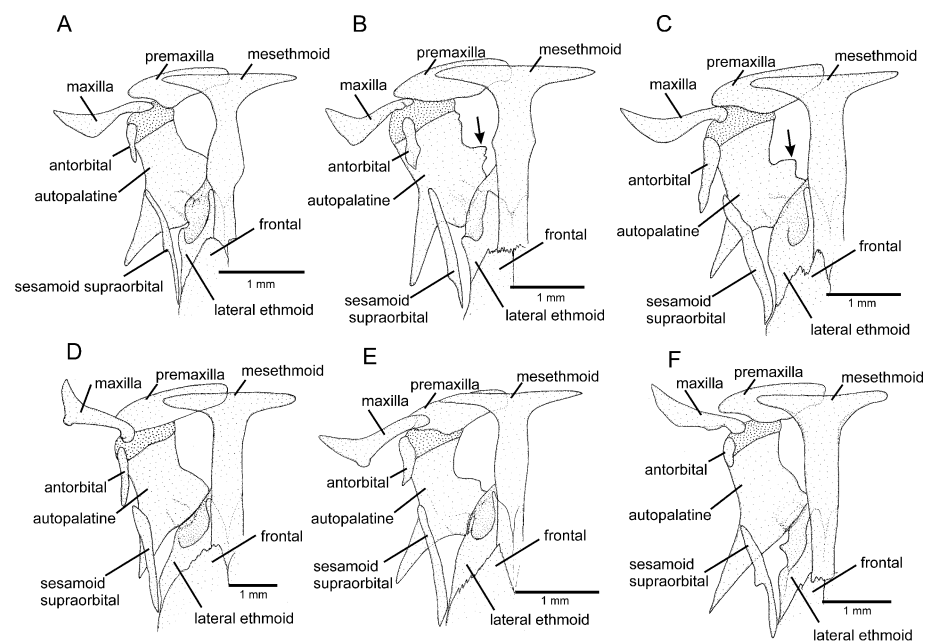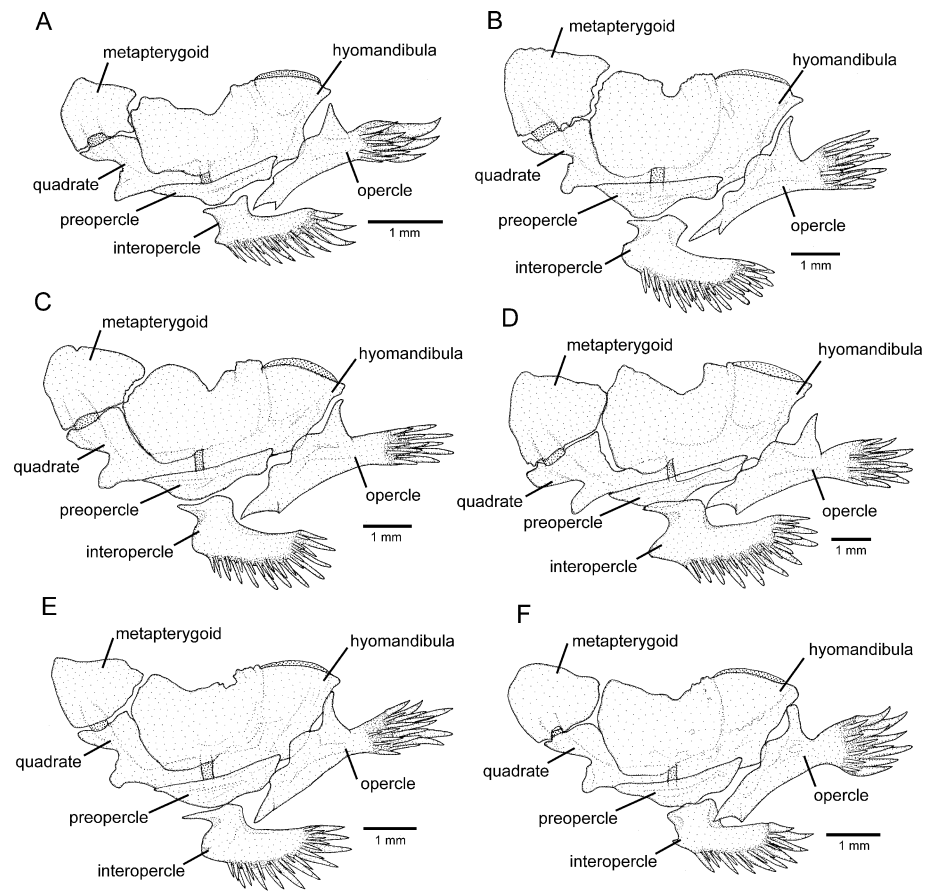**Figure 8.** Left jaw suspensorium and opercular series, lateral view: (**A**) *Cambeva* cf. *botuvera*; (**B**) *Cambeva chrysornata* sp. nov.; (**C**) *Cambeva cubataonis*; (**D**) *Cambeva guaratuba* sp. nov.; (**E**) *Cambeva ventropapillata* sp. nov.; (**F**) *Cambeva biseriata* sp. nov. Larger stippling represents cartilage.
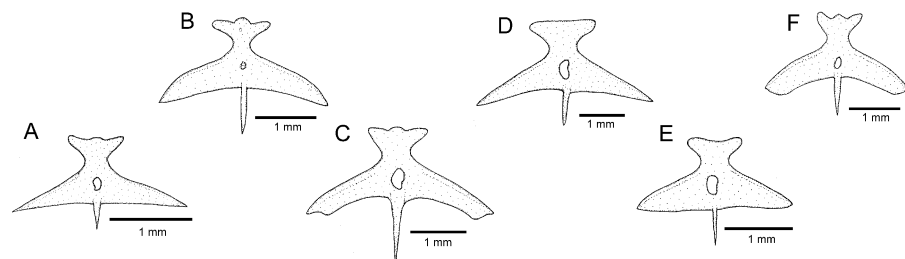

Figure 9. Parurohyal, ventral view, (**A**) *Cambeva* cf. *botuvera*; (**B**) *Cambeva chrysornata* sp. nov.; (**C**) *Cambeva cubataonis*; (**D**) *Cambeva guaratuba* sp. nov.; (**E**) *Cambeva ventropapillata* sp. nov.; (**F**) *Cambeva biseriata* sp. nov.

Populations of *C.* cf. *botuvera* from GBIA were formerly misidentified as *C. cubataonis* by Katz & Barbosa [55]. In the Rio Cubatão do Norte basin, both species occur in sympatry and can be misidentified because of the similar colour pattern and fin morphology, although *C.* cf. *botuvera* usually has paler colours. In this basin, *C.* cf. *botuvera* is distinguishable from *C. cubataonis* by the absence of the anterior infraorbital canal (vs. presence) and by having fewer vertebrae (36 or 37 vs. 40 or 41), fewer ribs (12 or 13 vs. 15 or 16), dorsal-fin origin at a vertical through the centrum of the 18th or 19th vertebra (vs. 21st); anal-fin origin at a vertical through the centrum of the 22nd or 23rd vertebra (vs. 25th or 26th); the autopalatine with a weakly concave medial margin (Figure 5A; vs. deeply concave, Figure 5B); and the lateral process of the parurohyal with straight posterior margin and

distally terminating in sharply pointed tip (Figure 6A; vs. curved posterior margin and truncate distal extremity, Figure 6B).

Distribution. *Cambeva* cf. *botuvera* was found in river basins draining into the Baía de Babitonga and Baía de Guaratuba, and in the Rio Itapocu basin (Figure 3).

Material examined. All from Brazil: Santa Catarina State. Baía de Guaratuba system: Rio São João basin: Garuva Municipality: UFRJ 13298, 1 ex. (C&S); UFRJ 13299, 3 exs.; Rio São João, 26°01′07″ S 48°50′56″ W, about 20 m asl; C. R. M. Feltrin, 25 July 2020. UFRJ 12908, 1 ex.; Rio Braço, 26°01′24″ S 48°51′44″ W, about 75 m asl; C. R. M. Feltrin & R. Dalcin, 16 April 2022. Baía de Babitonga system: Rio Três Barras basin: Garuva Municipality: UFRJ 13006, 8 ex.; Rio Três Barras, 26°05′40″ S 48°53′04″ W, about 20 m asl; C. R. M. Feltrin, 26 June 2022. Rio Cubatão do Norte basin: Joinville Municipality: UFRJ 8736, 16 ex.; UFRJ 8871, 3 ex. (C&S); Rio Lindo, tributary of the Rio Cubatão do Norte, 26°11′48″ S 48°55′19″ W, about 30 m asl; A. M. Katz et al., 29 May 2012. UFRJ 12886, 1 ex; middle course of the Rio Cubatão do Norte, Quiriri de Baixo, 26°08′35″ S 48°59′43″ W, about 35 m; C. R. M. Feltrin, 17 April 2022. UFRJ 12891, 1 ex.; UFRJ 12914, 1 ex; Rio Alandaf, Pirabeiraba, 26°13′00″ S 48°54′56″ W, about 35 m asl; C. R. M. Feltrin, 17 April 2022. UFRJ 12882, 11 ex.; UFRJ 12873, 5 ex.; Rio Lindo, Pirabeiraba, 26°11′49″ S 48°55′18″ W, about 30 m asl; C. R. M. Feltrin, 15 April 2022. UFRJ 10631, 2 ex; Rio Pirabeiraba, 26°08′42″ S 48°54′25″ W, about 30 m asl; A. Katz et al., 11 June 2015. UFRJ 12889, 2 ex; Rio Cubatão do Norte, Quiriri de Baixo, 26°08′35″ S 48°59′44″ W, about 55 m asl; C. R. M. Feltrin, 17 April 2022. UFRJ 12971, 1 ex; Rio Quiriri, 26°07′48″ S 49°00′32″ W, about 95 m asl; R. Dalcin, 15 April 2021. UFRJ 13008, 13 ex; UFRJ 13010, 1 ex.; stream tributary of Rio Quiriri, Quiriri de Baixo, 26°06′59″ S 49°00′11″ W, about 110 m asl; C. R. M. Feltrin, 26 July 2022. UFRJ 13214, 4 ex.; middle course of Rio Cubatão do Norte, Quiriri de Baixo, 26°08′35″ S 48°59′43″ W, about 35 m; C. R. M. Feltrin, 6 November 2020. UFRJ 13268, 2 ex.; Rio Quiriri, 26°15′50″ S 48°58′50″ W, about 85 m asl; R. Dalcin, 15 April 2021. UFRJ 12880, 3 ex.; same locality and collector as UFRJ 13214, 15 April 2019. UFRJ 13269, 18 ex.; Rio Cubatão do Norte, 26°08′48″ S 49°00′44″ W, about 95 m asl; C. R. M. Feltrin, 26 July 2022. MHNCI 11110, 2 ex.; Rio da Serra, a tributary of Rio Quiriri, Alto Quiriri, 49°00′33″ W 26°06′01″ S, V. Abilhoa, L.F. Duboc, L.P. Bastos & G. Otto, 20 April 2004. MHNCI 11057, 2 ex.; Rio Quiriri, Alto Quiriri, 49°00′12″ W 26°06′08″ S, V. Abilhoa, L.F. Duboc, L.P. Bastos, G. Otto, 20 April 2004. Rio Itapocu basin: Schroeder Municipality: UFRJ 12885, 8 ex; UFRJ 12870, 2 ex.; Rio Hern, tributary of Rio Itapocuzinho, Schroeder city, 26°25′33″ S 49°03′57″ W, about 35 m asl; C. R. M. Feltrin, 15 April 2022. UFRJ 12884, 1 ex; Rio Braço do Sul, tributary of Rio Itapocuzinho, 26°22′29″ S 49°03′52″ W, about 50 m asl; C. R. M. Feltrin, 19 January 2022. Corupá Municipality: UFRJ 12627, 7 ex.; Rio Novo, 26°25′37″ S 49°17′42″ W, about 120 m asl; C. R. M. Feltrin, 20 December 2019. UFRJ 13195, 2 ex; UFRJ 13196, 2 ex; Rio Isabel, tributary of Rio Novo, 26°28′45″ S 49°18′16″ W, about 165 m asl; C. R. M. Feltrin, 15 April 2022. UFRJ 13191, 4 ex.; UFRJ 13190, 2 ex.; Rio Paulo Grande, tributary to Rio Isabel, tributary of Rio Novo, 26°26′52″ S 49°17′31″ W, about 110 m; C. R. M. Feltrin, 30 August 2022. UFRJ 13193, 4 ex.; UFRJ 13194, 10 ex.; stream tributary of Rio Isabel, tributary of Rio Novo, 26°28′18″ S 49°17′56″ W, about 150 m asl; C. R. M. Feltrin, 17 April 2022. UFRJ 13201, 5 ex.; UFRJ 13202, 2 ex.; Rio Humboldt, Osvaldo Amaral, 26°23′21″ S 49°15′12″ W, about 90 m; C. R. M. Feltrin, 29 December 2022. UFRJ 13192, 2 ex.; Rio Paulo Pequeno, tributary of Rio Paulo Grande, tributary of Rio Isabel, tributary of Rio Novo, 26°27′11″ S 49°18′29″ W, about 115 m asl; C. R. M. Feltrin, 30 August 2022. UFRJ 12861, 4 ex.; upper Rio Itapocu, João Tozini, 26°26′17″ S 49°13′21″ W, about 35 m asl; C. R. M. Feltrin, 15 April 2022. UFRJ 13218, 3 ex. (C&S); UFRJ 13219, 15 ex.; UFRJ 13216, 2 ex. (C&S); same locality and collector as UFRJ 12861, 26 November 2020. UFRJ 12865, 8 ex; Rio Novo, 26°25′51″ S 49°16′47″ W, about 95 m SL; C. R. M. Feltrin, 15 April 2022. Jaraguá do Sul Municipality: UFRJ 12907, 5 ex., stream at the city of Jaraguá do Sul, SC, 26°29′38″ S 49°04′10″ W, about 30 m asl; C. R. M. Feltrin, 15 April 2022. UFRJ 12903, 1 ex; UFRJ 12864, 1 ex.; Ribeirão Cavalo, tributary of the upper Rio Itapocu, 26°27′43″ S 49°11′03″ W, about 80 m asl; C. R. M. Feltrin, 15 April 2022. UFRJ 12862, 2 ex.; UFRJ 12888, 3 ex.; Rio Cerro, 26°33′21″ S 49°08′01″

W, about 50 m asl; C. R. M. Feltrin, 15 April 2022. Massaranduba Municipality: UFRJ 12902, 2 ex; UFRJ 12874, 2 ex.; Rio Sete de Janeiro, 26°39′40″ S 49°00′46″ W, about 80 m asl; C. R. M. Feltrin, 15 April 2022. UFRJ 13209, 11 ex.; Ribeirão Treze de Maio, tributary of Rio Massaranduba; 26°39′42″ S 49°02′01″ W, about 70 m asl; 15 April 2022.

Cambeva chrysornata sp. nov.

LSID:urn:lsid:zoobank.org:act:B69BBE4B-8FD5-4878-BFDC-45EF4F28C627

Cambeva cubataonis (non *Trichomycterus cubataonis* Bizerril, 1994): Donin, Ferrer & Carvalho [30] (Figure 6C–E in Ref. [30]) (misidentification).

Figure 7B, Figure 8B, Figure 9B, Figure 10 and Table 1, respectively.

Figure 10. *Cambeva chrysornata* sp. nov., UFRJ 13011, holotype, 94.5 mm SL: (**A**) lateral, (**B**) dorsal, and (**C**) ventral views.

Table 1. Morphometric data of *Cambeva chrysornata* sp. nov.

	Holotype	Paratypes (n = 4)
Standard length (SL)	94.5	42.7–71.4
Percentage of standard length		
Body depth	13.9	15.5–17.5
Caudal peduncle depth	10.9	12.5–13.6
Body width	12.6	11.8–13.9
Caudal peduncle width	5.2	4.7–6.3
Pre-dorsal length	63.1	61.5–66.4
Pre-pelvic length	56.3	56.7–59.6
Dorsal-fin base length	11.0	10.8–12.9
Anal-fin base length	7.9	9.3–10.0
Caudal-fin length	10.6	12.2–15.6
Pectoral-fin length	9.1	9.8–13.0
Pelvic-fin length	7.9	7.6–9.4
Head length	19.7	19.7–23.2
Percentage of head length		
Head depth	47.2	46.2–50.9
Head width	85.2	77.6–91.3
Snout length	39.5	36.7–40.6
Interorbital width	19.6	19.7–25.7
Preorbital length	15.2	12.3–14.2
Eye diameter	7.4	7.7–10.5

Holotype. UFRJ 13011, 94.5 mm SL; Brazil: Santa Catarina State: Garuva Municipality: a stream tributary of Rio Palmital, Baía de Babitonga system, near the centre of the town of Garuva, 26°02′05″ S 48°51′28″ W, about 35 m asl; C. R. M. Feltrin, 25 June 2022.

Paratypes. UFRJ 12899, 3 ex., 30.0–71.4 mm SL; UFRJ 13017, 2 ex., 42.7–65.1 mm SL (C&S); UFRJ 12860, 1 ex., 38.2 mm SL (DNA); CICCAA 07549, 1 ex., 42.9 mm SL; same locality as holotype; C. R. M. Feltrin and R. H. Dalcin, 16 April 2022.

Diagnosis. *Cambeva chrysornata* is distinguished from all other congeners, except *C. cubataonis* and *C. guaratuba*, by adult specimens above about 40 mm SL, having flank and dorsum predominantly dark grey to black contrasting with bright yellow marks (vs. never a similar colour pattern) and the presence of odontodes with a rounded extremity at least on the internal-most series of the interopercle in specimens above about 60 mm SL (vs. pointed odontodes). *Cambeva chrysornata* is distinguished from *C. cubataonis* and *C. guaratuba* by having shorter barbels, the tip of the rictal barbel posteriorly reaching the anterior margin of the orbit or an area anterior to it (vs. reaching area posterior to the orbit) and maxillary and rictal barbels not reaching interopercular patch of odontodes (vs. reaching interopercular patch of odontodes), a slender dorsal fin with short rays, with the longest ray shorter than the dorsal-fin base (vs. longest ray longer than the dorsal-fin base), pectoral fin rounded in dorsal view (vs. subtriangular), pelvic fin rounded, its posterior extremity reaching a vertical anterior to the dorsal-fin origin (vs. truncate, its posterior extremity reaching a vertical through the anterior half of the dorsal-fin base), fewer procurrent caudal-fin rays (total of 16 or 17 dorsally and 11 or 12 ventrally, vs. 20 or 21 dorsally and 13 or 14 ventrally), fewer vertebrae (38 or 39, vs. 40 or 41), and the presence of an irregularly shaped golden longitudinal line on the medio-dorsal portion of the flank (vs. no distinctive golden longitudinal line on the medio-dorsal portion of the flank). *Cambeva chrysornata* is similar to *C. cubataonis* and is distinguished from *C. guaratuba* by the medial margin of the autopalatine exhibiting a deep concavity in its middle portion, posteriorly followed by a distinctive projection towards the mesethmoid. *Cambeva chrysornata* is also distinguished from *C. cubataonis* by having 14 vertebrae (vs. 15–16).

Description. General morphology: Morphometric data are presented in Table 1. Body relatively slender, subcylindrical on anterior region, compressed on posterior region. Greatest body depth in area immediately anterior to pelvic-fin base. Dorsal profile slightly convex between snout and dorsal-fin base end, nearly straight on caudal peduncle; ventral profile convex on head, approximately straight on trunk. Anus and urogenital papilla opening at vertical through middle portion of dorsal-fin base. Head sub-trapezoidal, with anterior profile of snout slightly convex in dorsal view. Eye small, dorsally positioned on head, nearer snout tip than posterior margin of opercle. Distance between anterior and posterior nostrils about half distance between posterior nostril and orbital rim. Barbels narrow and short, tip of nasal barbel posteriorly reaching orbit, tip of maxillary and rictal barbels reaching area anterior to interopercular patch of odontodes. Mouth subterminal. Lateral fleshy lobe of the mouth small, its largest length about one-fourth of lower jaw length excluding lobes; ventral surface of lobe flat. Jaw teeth irregularly arranged, more external teeth longer, incisiform in specimens above about 50 mm SL, with rounded extremity in smaller specimens, more internal teeth pointed, 40–54 on premaxilla, 41–66 on dentary. Minute skin papillae on ventral surface of head, including lateral lobe of mouth, and dorso-lateral surface of snout. Branchial membrane attached to isthmus only at its anterior-most point, in ventral midline.

Dorsal and anal fins subtriangular, margin rounded, dorsal fin slender, rays short, longest ray shorter than fin base. Total dorsal-fin rays 11 (ii + II + 7), total anal-fin rays 9 (ii + II + 5). Anal-fin origin at posterior portion to dorsal-fin base. Dorsal-fin origin at vertical through centrum of 20th or 21st vertebra; anal-fin origin at vertical through centrum of 24th or 25th vertebra. Pectoral fin rounded in dorsal view, first pectoral-fin ray shorter than second ray, not forming terminal filament. Total pectoral-fin rays 7 (I + 6). Pelvic fin rounded, its posterior extremity in vertical anterior to dorsal-fin origin. Pelvic-fin bases medially separated by minute interspace. Total pelvic-fin rays 5 (I + 4). Caudal fin

subtruncate, posterior corners rounded. Total principal caudal-fin rays 13 (I + 11 + I), total dorsal procurrent rays 16 or 17 (xv–xvi + I), total ventral procurrent rays 10 or 11 (ix–x + I).

Laterosensory system: Supraorbital, posterior section of infraorbital canal and postorbital canal continuous. Supraorbital sensory canal pores 3: s1, adjacent to medial margin of anterior nostril; s3, adjacent and just posterior to medial margin of posterior nostril; s6, in transverse line through posterior half of orbit; pore s6 slightly nearer orbit than its paired s6 homologous pore. Anterior infraorbital sensory canal pores 2: i1, at transverse line through anterior nostril, and i3, at transverse line just anterior to posterior nostril. Posterior infraorbital sensory canal pores 2: pore i10, adjacent to ventral margin of orbit, and pore i11, posterior to orbit. Postorbital canal pores 2: po1, at vertical through posterior portion of interopercular patch of odontodes, and po2, at vertical through posterior portion of opercular patch of odontodes. Lateral line pores 2; posterior-most pore at vertical just posterior to pectoral-fin base.

Osteology: Mesethmoid thin, anterior margin straight to slightly convex, lateral margin with small projection just anterior to lateral ethmoid. Mesethmoid cornu narrow, tip rounded. Postero-lateral area of lateral ethmoid with pronounced projection. Antorbital thin, sub-elliptical, about half length of premaxilla. Sesamoid supraorbital slender, flat, with small postero-lateral projection, its length about two and half times antorbital length. Premaxilla sub-trapezoidal in dorsal view, laterally narrowing, longer than maxilla. Maxilla curved, about L-shaped. Autopalatine sub-rectangular in dorsal view when excluding its postero-lateral process, its largest width about two-thirds of its length, including anterior cartilage; medial margin sinuous, with deep concavity in middle portion, posteriorly followed by distinctive projection towards mesethmoid. Autopalatine posterolateral process well-developed, its length about equal to autopalatine length without anterior cartilage. Metapterygoid thin, longer than deep. Quadrate slender, dorsal process with constricted base, dorsoposterior margin in contact with hyomandibula outgrowth. Hyomandibula long, with well-developed anterior outgrowth; dorsal margin of hyomandibula outgrowth with shallow concavity. Opercle long, longer than interopercle; opercular odontode patch robust, its width about three-fourths of dorsal hyomandibula articular facet. Opercular odontodes 18, irregularly arranged, narrow, nearly straight. Dorsal process of opercle short, slightly curved, extremity rounded. Opercular articular facet for hyomandibula with rounded flap, articular facet for preopercle small, about half size of articular facet for hyomandibula, rounded. Interopercle moderate in length, about equal to hyomandibula outgrow horizontal length, with rounded anterior margin. Interopercular odontodes 30 or 31, nearly straight, larger odontodes as long as larger opercular odontodes, irregularly arranged; in specimens above about 50 mm SL, posterior odontodes with rounded tip, anterior odontodes pointed, in smaller specimens, odontodes always pointed. Preopercle compact, with minute ventral projection. Parurohyal robust, lateral process slightly curved. Parurohyal head well-developed, with prominent anterolateral paired process. Middle parurohyal foramen minute. Posterior process of parurohyal moderately long, about three-fourths distance between anterior margin of parurohyal and anterior insertion of posterior process. Branchiostegal rays 8 or 9. Vertebrae 38 or 39. Ribs 14. Two dorsal hypural plates corresponding to hypurals 3 + 4 + 5; single ventral hypural plate corresponding to hypurals 1 + 2 and parhypural.

Colouration in alcohol: Flank, dorsum and head side dark grey to brown, darker on dorsal portion, with irregularly shaped yellow reticulation, more diffused ventrally on flank and head, usually forming pale golden longitudinal line along medio-dorsal portion of flank, between area just posterior to head and area below dorsal-fin base, sometimes interrupted or with dorsal extensions. Venter and ventral surface of head white. Barbels grey. Fins hyaline with white basal portion, sometimes with dark chromatophores forming pale grey dots. Smallest specimen (30.0 mm SL), body homogeneously pale grey, with broad longitudinal dark grey band along dorsal portion of flank.

Etymology. From the Greek *chrysos* (gold) and the Latin *ornata* (ornate), an allusion to the characteristic bright yellow marks on the flank of the new species.

Distribution and habitat notes. Cambeva chrysornata is only known from a single locality, a stream tributary of the upper Rio Palmital basin, which is the northern-most basin of the Baía de Babitonga basin, altitude about 35 m asl (Figure 4). Different sections of the basin were sampled, including the Rio da Anta, Rio da Onça and Rio Três Barras, but *C. chrysornata* was only found at the type locality site, where the species was rare. The type locality is situated within the urban area of the city of Garuva. While sampling the stream along about 2 km above the type locality, discharges of domestic effluents such as detergents, coliforms, oils and hydrocarbons were recorded. Below the type locality, the hydrographic basin is highly modified, crossing the city. Marginal vegetation comprises a narrow zone of degraded riparian forest. At the type locality, the stream is about 1.5 to 5 m wide and about 0.05 to 1 m deep. Most type specimens were found below median to large sized stones, about 0.4 m of diameter, but smaller specimens were found below smaller pebbles, about 0.05 to 0.15 m of diameter, and the two largest specimens under leaf litter below a large stone about 0.70 m of diameter.

Cambeva cubataonis (Bizerril, 1994)

Trichomycterus cubataonis Bizerril, 1994 [23] (p. 618).
Cambeva cubataonis (Bizerril): Katz et al. [21] (p. 563) (new combination).
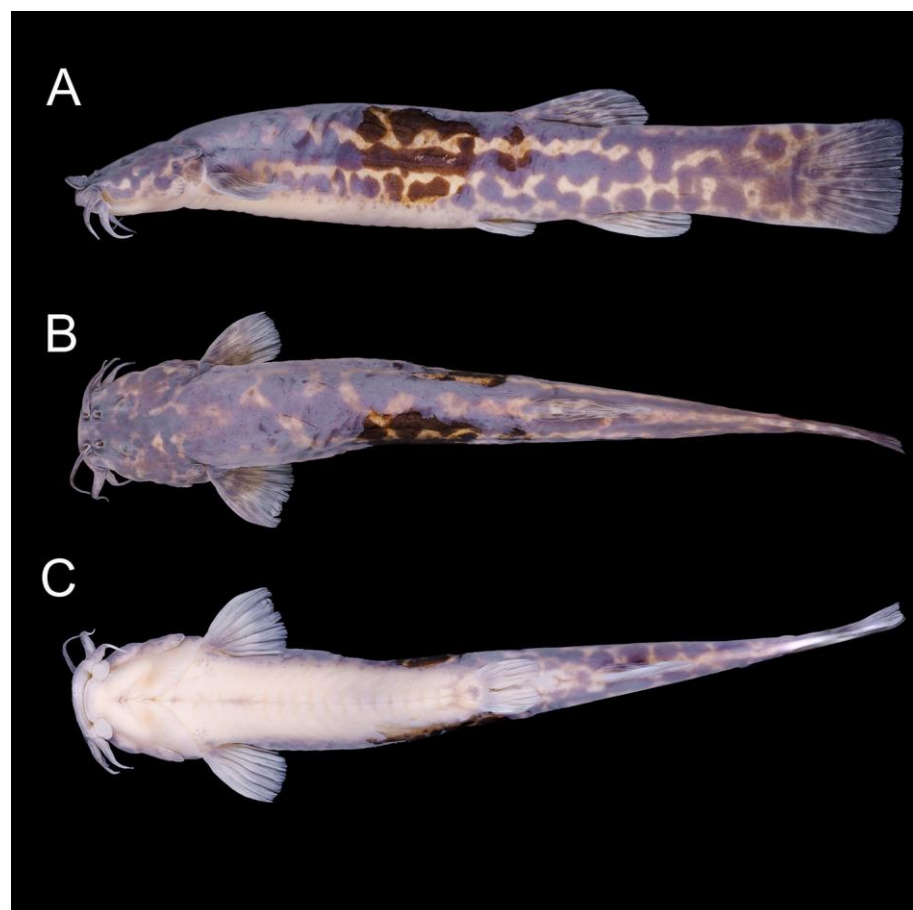Figures 7C, 8C, 9C and 11, respectively.

Figure 11. *Cambeva cubataonis*, UFRJ 13189, Rio Cubatão do Norte basin, 70.8 mm SL: (**A**) lateral, (**B**) dorsal, and (**C**) ventral views.

Diagnosis. Cambeva cubataonis is distinguished from all other congeners, except *C. chrysornata* and *C. guaratuba*, by adult specimens above about 40 mm SL, having flank and dorsum predominantly dark grey to black contrasting with bright yellow marks (vs. never a similar colour pattern) and the presence of odontodes with a rounded extremity at least

on the internal-most series of the interopercle in larger specimens, above about 60 mm SL (vs. always pointed odontodes). *Cambeva cubataonis* is distinguished from *C. chrysornata* and *C. guaratuba* by having 15 or 16 ribs (vs. 14) and a relatively longer posterior process of the parurohyal, its length longer that the length between the anterior margin of the parurohyal and the anterior insertion of the posterior process. *Cambeva cubataonis* is also distinguished from *C. chrysornata* by having longer barbels, the tip of the rictal barbel posteriorly reaching area posterior to the orbit (vs. reaching the anterior margin of the orbit or an area anterior to it) and maxillary and rictal barbels reaching interopercular patch of odontodes (vs. not reaching), a relatively deep dorsal fin, with the longest ray longer than the dorsal-fin base (vs. longest ray shorter than the dorsal-fin base), pectoral fin subtriangular in dorsal view (vs. rounded), pelvic fin truncate, its posterior extremity reaching a vertical at the anterior half of the dorsal-fin base (vs. rounded, its posterior extremity reaching a vertical anterior to the dorsal-fin origin), more procurrent caudal-fin rays (total of 20 or 21 dorsally and 13 or 14 ventrally, vs. 16 or 17 dorsally and 11 or 12 ventrally), more vertebrae (40 or 41, vs. 38 or 39), and the absence of an irregularly shaped golden longitudinal line on the medio-dorsal portion of the flank (vs. presence). *Cambeva cubataonis* is also distinguished from *C. guaratuba* by having jaw teeth with pointed to rounded tip, irregularly arranged (vs. truncate to slightly bilobed teeth, arranged in three rows), more opercular odontodes (18–20, vs. 13–16), and presence of a distinctive projection on the posterior portion of the medial margin of the autopalatine (vs. absence).

Distribution and ecological notes. Cambeva cubataonis presently is known only from the type locality area, in the Rio Cubatão do Norte basin, Baía de Babitonga system, in altitudes between about 45 and 110 m asl (Figure 3). It was mostly found both in the middle main channel of the Rio Cubatão do Norte and in the Rio Quiriri, rarely being collected in tributary streams. Their preference for microhabitats follows that described for most congeners, with smaller specimens found below small pebbles, between about 0.01 and 0.15 m, and larger specimens in pebbles of greater diameters, about 0.25 m or more. The Rio Cubatão do Norte river, in the stretches where *C. cubataonis* occurs, has an average width of about 35 m and deepest areas with 1.2 m. In the Rio Quiriri, the locality where *C. cubataonis* was found is about 20 m wide and about 0.8 m at the deepest points. At both areas, the marginal forest is still relatively well preserved.

Material examined. All localities in Brazil: Santa Catarina State: Joinville Municipality: Rio Cubatão do Norte basin, Baía de Babitonga system: MNRJ 12490, holotype; middle Rio Cubatão do Norte; C. R. S. F. Bizerril & P. M. C. Araújo, 10 November 1991. UFRJ 13212, 1; UFRJ 13213, 1 (C&S); small tributary of the middle Rio Cubatão do Norte, Baía de Babitonga system, Quiriri de Baixo, 26°08′35″ S 48°59′44″ W, about 75 m asl; C. R. M. Feltrin, 6 November 2020. UFRJ 13189, 1; same locality and collector, 26 July 2022. UFRJ 13167, 8 (DNA); same locality and collector, 24 September 2022. UFRJ 13267, 2 ex., Rio Quiriri, 26°07′14″ S 49°00′14″ W, about 110 m asl; R. Dalcin, 15 April 2015. UFRJ 12978, 4; UFRJ 12972, 2 (C&S); same locality and collector as UFRJ 13267, 15 April 2021.

Cambeva guaratuba sp. nov.

LSID:urn:lsid:zoobank.org:act:DF384344-8118-4CD5-8965-6C1728CE209C

Cambeva cubataonis (non *Trichomycterus cubataonis* Bizerril, 1994): Donin et al. [30] (Figure 6A,B in Ref. [30]) (misidentification).

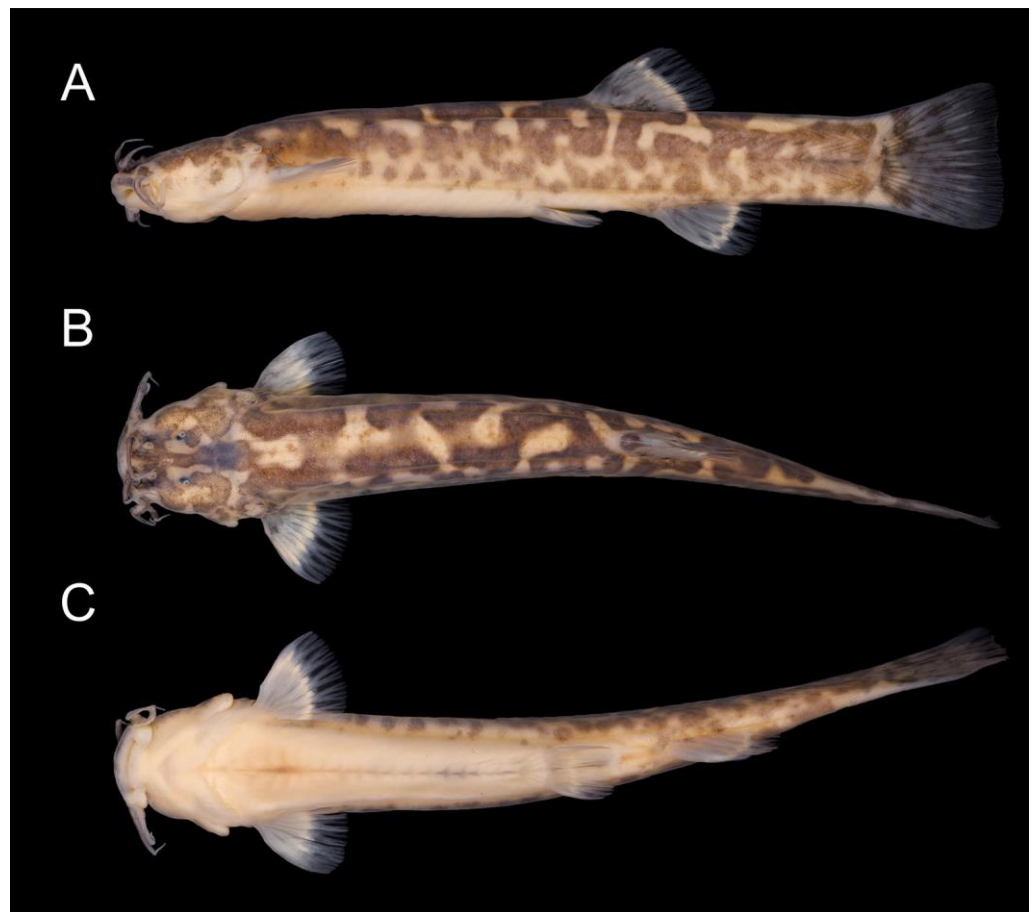Figure 7D, Figure 8D, Figure 9D, Figure 12 and Table 2, respectively.

Figure 12. *Cambeva guaratuba* sp. nov., UFRJ 13296, holotype, 63.6 mm SL: (**A**) lateral, (**B**) dorsal, and (**C**) ventral views.

Table 2. Morphometric data of *Cambeva guaratuba* sp. nov.

	Holotype	**Paratypes (n = 3)**
Standard length (SL)	63.6	63.0–82.2
Percentage of standard length		
Body depth	14.8	14.4–15.0
Caudal peduncle depth	11.7	10.5–12.2
Body width	12.0	10.0–10.9
Caudal peduncle width	4.7	3.4–4.2
Pre-dorsal length	61.4	60.4–63.3
Pre-pelvic length	56.0	54.4–58.6
Dorsal-fin base length	11.3	11.8–12.9
Anal-fin base length	9.2	9.6–10.3
Caudal-fin length	16.1	12.1–16.8
Pectoral-fin length	12.2	10.6–13.7
Pelvic-fin length	8.8	7.9–9.8
Head length	19.6	20.1–21.3
Percentage of head length		
Head depth	47.4	42.1–50.4
Head width	82.5	77.5–79.6
Snout length	41.4	38.8–42.2
Interorbital width	23.6	19.1–23.5
Preorbital length	14.6	14.0–14.4
Eye diameter	9.5	7.9–9.4

Holotype. UFRJ 13296, 63.6 mm SL; Brazil: Paraná State: Guaratuba Municipality: Rio Imbira, a tributary of Rio São João, Baía de Guaratuba system, 25°57′31″ S 48°53′58″ W, about 105 m asl; C. R. M. Feltrin, 25 June 2022.

Paratypes. All from Brazil: UFRJ 13007, 6 ex., 28.1–63.0 mm SL; collected with the holotype. Santa Catarina State: Garuva Municipality: UFRJ 12302, 1 ex. (DNA), 49.6 mm SL; UFRJ 12303, 2 ex. (C&S), 27.5–82.2 mm SL; Rio São João, 26°01′22″ S 48°51′41″ W, about 70 m asl; R. Dalcin, 19 April 2014. CICCAA 07550, 1 ex., 67.9 mm SL; same locality as UFRJ 12302; R. Dalcin, 15 September 2019.

Diagnosis: *Cambeva guaratuba* is distinguished from all other congeners, except *C. chrysornata* and *C. cubataonis*, by adult specimens, above about 40 mm SL, having flank and dorsum predominantly dark grey to black contrasting with bright yellow marks (vs. never a similar colour pattern) and the presence of odontodes with a rounded extremity at least on the internal-most series of the interopercle in larger specimens, above about 60 mm SL (vs. pointed odontodes). *Cambeva guaratuba* is distinguished from *C. chrysornata* and *C. cubataonis* by having truncate to slightly bilobed jaw teeth, arranged in three rows (vs. teeth with pointed to rounded tip, irregularly arranged), fewer opercular odontodes (13–16, vs. 18–20), and absence of a distinctive projection on the posterior portion of the medial margin of the autopalatine (vs. presence). *Cambeva guaratuba* is also distinguished from *C. chrysornata* by having longer barbels, the tip of the rictal barbel posteriorly reaching area posterior to the orbit (vs. reaching the anterior margin of the orbit or an area anterior to it) and maxillary and rictal barbels reaching interopercular patch of odontodes (vs. not reaching), a relatively deep dorsal fin, with the longest ray longer than the dorsal-fin base (vs. longest ray shorter than the dorsal-fin base), pectoral fin subtriangular in dorsal view (vs. rounded), pelvic fin truncate, its posterior extremity reaching a vertical at the anterior half of the dorsal-fin base (vs. rounded, its posterior extremity reaching a vertical anterior to the dorsal-fin origin), more procurrent caudal-fin rays (total of 20 or 21 dorsally and 13 or 14 ventrally, vs. 16 or 17 dorsally and 11 or 12 ventrally), more vertebrae (40 or 41, vs. 38 or 39), and the absence of an irregularly shaped golden longitudinal line on the medio-dorsal portion of the flank (vs. presence). *Cambeva guaratuba* is also distinguished from *C. cubataonis* by having 14 vertebrae (vs. 15–16).

Description. General morphology: Morphometric data are presented in Table 2. Body relatively slender, subcylindrical on anterior region, compressed on posterior region. Greatest body depth in area immediately anterior to pelvic-fin base. Dorsal profile slightly convex between snout and dorsal-fin base end, nearly straight on caudal peduncle; ventral profile convex on head, approximately straight on trunk. Anus and urogenital papilla opening at vertical through area just anterior to middle of dorsal-fin base. Head sub-trapezoidal, with anterior profile of snout slightly convex in dorsal view. Eye small, dorsally positioned on head, nearer snout tip than posterior margin of opercle. Distance between anterior and posterior nostrils about half distance between posterior nostril and orbital rim. Barbels narrow, moderate in length, tip of nasal barbel reaching area between orbit and opercular patch of odontodes, tip of maxillary barbel reaching posterior portion of interopercular patch of odontodes, rictal barbel reaching middle portion of interopercular patch of odontodes. Mouth subterminal. Lateral fleshy lobe of the mouth small, its largest length about one fourth of lower jaw length excluding lobes; ventral surface of lobe flat. Jaw teeth incisiform, sometimes slightly bilobed in specimens above about 50 mm SL, pointed in smaller specimens, 38–40 on premaxilla, 38–43 on dentary. Minute skin papillae on ventral surface of head, including lateral lobe of mouth, and dorso-lateral surface of snout. Branchial membrane attached to isthmus only at its anterior-most point, in ventral midline.

Dorsal and anal fins subtriangular, anterior margin straight, posterior margin slightly convex, longest ray longer than fin base. Total dorsal-fin rays 11 (ii + II + 7), total anal-fin rays 9 (ii + II + 5). Anal-fin origin at posterior portion to dorsal-fin base, at vertical through base of fifth bifid ray. Dorsal-fin origin at vertical through centrum of 20th vertebra; anal-fin origin at vertical through centrum of 24th vertebra. Pectoral fin subtriangular in dorsal view, first pectoral-fin ray shorter than second ray, not forming terminal filament. Total pectoral-

fin rays 7 (I + 6). Pelvic fin truncate, its posterior extremity at vertical through anterior portion of dorsal-fin base. Pelvic-fin bases medially in close proximity. Total pelvic-fin rays 5 (I + 4). Caudal fin subtruncate, posterior corners rounded. Total principal caudal-fin rays 13 (I + 11 + I), total dorsal procurrent rays 20 (xix + I), total ventral procurrent rays 13 or 14 (xii–xiii + I)

Laterosensory system: Supraorbital, posterior section of infraorbital canal and postorbital canal continuous. Supraorbital sensory canal pores 3: s1, adjacent to medial margin of anterior nostril; s3, adjacent and just posterior to medial margin of posterior nostril; s6, in transverse line through posterior half of orbit; pore s6 slightly nearer orbit than its paired s6 homologous pore. Anterior infraorbital sensory canal pores 2: i1, at transverse line through anterior nostril, and i3, at transverse line just anterior to posterior nostril. Posterior infraorbital sensory canal pores 2: pore i10, adjacent to ventral margin of orbit, and pore i11, posterior to orbit. Postorbital canal pores 2: po1, at vertical through posterior portion of interopercular patch of odontodes, and po2, at vertical through posterior portion of opercular patch of odontodes. Lateral line pores 2; posterior-most pore at vertical just posterior to pectoral-fin base.

Osteology: Mesethmoid thin, anterior margin approximately straight, lateral margin without projections. Mesethmoid cornu narrow, tip rounded. No distinctive projection on lateral surface of lateral ethmoid. Antorbital thin, elongate, about half length of premaxilla. Sesamoid supraorbital slender, flat, without lateral projections, its length about two times antorbital length. Premaxilla sub-trapezoidal in dorsal view, longer than maxilla. Maxilla curved, boomerang-shaped. Autopalatine sub-rectangular in dorsal view when excluding its postero-lateral process, its largest width about three fourths of its length, including anterior cartilage; medial margin with pronounced concavity, lateral margin slightly concave. Autopalatine posterolateral process well-developed, triangular in dorsal view, its length about two-thirds of autopalatine length. Metapterygoid thin, longer than deep. Quadrate slender, dorsal process with constricted base, dorsoposterior margin in contact with hyomandibula outgrowth. Hyomandibula long, with well-developed anterior outgrowth; dorsal margin of hyomandibula outgrowth with shallow concavity. Opercle long, longer than interopercle; opercular odontode patch robust, its width about three fourths of dorsal hyomandibula articular facet. Opercular odontodes 13–16, irregularly arranged, narrow, nearly straight, with rounded to slightly pointed extremity. Dorsal process of opercle short, extremity pointed. Opercular articular facet for hyomandibula with rounded flap, articular facet for preopercle slightly smaller than articular facet for hyomandibula, rounded. Interopercle moderate in length, about equal to hyomandibula outgrow horizontal length, with prominent expansion on anterior margin. Interopercular odontodes 28–32, nearly straight, larger odontodes as long as larger opercular odontodes, irregularly arranged; in specimens above about 50 mm SL, posterior odontodes with rounded tip, anterior odontodes pointed, in smaller specimens, odontodes always pointed. Preopercle compact, with minute ventral projection. Parurohyal robust, lateral process triangular, posterior margin about straight. Parurohyal head well-developed, with prominent anterolateral paired process. Middle parurohyal oval. Posterior process of parurohyal short, about half distance between anterior margin of parurohyal and anterior insertion of posterior process. Branchiostegal rays 8. Vertebrae 40. Ribs 14. Two dorsal hypural plates corresponding to hypurals 3 + 4 + 5; single ventral hypural plate corresponding to hypurals 1 + 2 and parhypural.

Colouration in alcohol: Flank, dorsum and head side dark grey to brown, with irregularly shaped yellow reticulation. Venter and ventral surface of head white. Barbels grey. Fins hyaline with dark chromatophores forming dark grey spots on basal region. In smallest specimens, about 30.0 mm SL, body pale grey with small brown spots.

Etymology. The name *guaratuba* is an allusion to the occurrence of the new species in the Baía de Guaratuba system, here used as a noun in apposition. From the Tupi-Guarani, the name *guaratuba* means *guara* (popular name of the bird *Eudocimus ruber* Linnaeus, 1758) and *tuba* (numerous), designating a place inhabited by numerous birds of this species.

Distribution and habitat notes. Cambeva guaratuba was found in localities of the Rio São João basin, which is connected to the Baía de Guaratuba system, in altitudes between about 70 and 105 m asl (Figure 3). At the type locality area, the Rio Imbira is a fast-flowing stream, between about 7 and 15 m wide, and about 1 m deep in the deepest areas, with the bottom substrate mostly comprising pebbles and stones, between about 0.01 and 0.6 of diameter. Larger specimens were found below larger stones, as well as, within tangles of marginal plant roots. The marginal forest is relatively well-preserved, and the water does not present vestiges of pollution. However, frequent accidents with freight trucks on the road adjacent to this drainage area, the BR-376 road, can have negative effects on water quality. In the last 12 years, 89 accidents with spillage of dangerous products occurred in the region. For example, in February 2022, a truck carrying 31,970 kg of residual 69% sulfuric acid overturned, spilling its entire load into a tributary of the São João River. The rarity of this species may be related to these accidents.

Cambeva ventropapillata sp. nov.

LSID:urn:lsid:zoobank.org:act:82C632F7-3A94-4DE4-96AE-8053DD857349

Trichomycterus nigricans (non *Trichomycterus nigricans* Valenciennes, 1832): de Pinna [56] (p. 227).

Figure 7E, Figure 8E, Figure 9E, Figure 13 and Table 3, respectively.

Figure 13. *Cambeva ventropapillata* sp. nov., UFRJ 13013, holotype, 75.3 mm SL: (**A**) lateral, (**B**) dorsal, and (**C**) ventral views.

Table 3. Morphometric data of *Cambeva ventropapillata* sp. nov.

	Holotype	**Paratypes (n = 10)**
Standard length (SL)	75.3	40.8–82.8
Percentage of standard length		
Body depth	13.4	14.0–17.0
Caudal peduncle depth	11.4	11.4–15.2
Body width	9.3	9.0–12.2
Caudal peduncle width	3.8	2.8–4.8

Table 3. *Cont.*

	Holotype	Paratypes (n = 10)
Pre-dorsal length	61.9	60.2–63.8
Pre-pelvic length	53.2	51.5–57.5
Dorsal-fin base length	11.0	10.9–12.2
Anal-fin base length	9.6	8.6–10.1
Caudal-fin length	15.4	14.5–17.9
Pectoral-fin length	12.6	11.3–14.3
Pelvic-fin length	9.0	7.4–10.0
Head length	18.9	18.6–22.0
Percentage of head length		
Head depth	44.3	43.8–56.5
Head width	77.1	74.6–85.4
Snout length	39.6	39.5–44.4
Interorbital width	24.2	19.4–26.3
Preorbital length	15.1	11.0–15.9
Eye diameter	9.2	9.5–12.8

Holotype. UFRJ 13013, 75.3 mm SL; Brazil: Santa Catarina State: Massaranduba Municipality: Ribeirão Treze de Maio, a tributary of Rio Massaranduba, itself a tributary of Rio Pitanga, Rio Itapocu basin, 26°39′42″ S 49°02′01″ W, about 75 m asl; C. R. M. Feltrin, 15 April 2022.

Paratypes. All from Brazil: Estado de Santa Catarina: Rio Itapocu basin. Massaranduba Municipality: UFRJ 12910, 5 ex., 35.7–39.5 mm SL; UFRJ 13016, 3 ex. (C&S), 40.8–54.7 mm SL; UFRJ 12859, 2 ex. (DNA), 34.6–38.4 mm SL; collected with holotype. Corupá Municipality: UFRJ 13295, 1 ex., 79.9 mm SL; Rio Novo, tributary of Rio Itapocu; C. R. M. Feltrin, 20 December 2019. UFRJ 13203, 2 ex., 63.3–72.7 mm SL; Rio Paulo Pequeno, tributary of Rio Paulo Grande, tributary of Rio Isabel, tributary of Rio Novo, 26°27′11″ S 49°18′29″ W, about 115 m asl; C. R. M. Feltrin, 8 December 2021. UFRJ 13220, 5 ex., 57.4–82.8 mm SL; UFRJ 13217, 1 ex. (C&S), 56.1 mm SL; upper Rio Itapocu, João Tozini, 26°26′17″ S 49°13′21″ W, about 35 m asl; C. R. M. Feltrin, 26 November 2020. UFRJ 13207, 1 ex., 56.9 mm SL; Rio Paulo Grande, tributary to Rio Isabel, tributary of Rio Novo, 26°26′52″ S 49°17′31″ W, about 110 m; C. R. M. Feltrin, 16 August 2022. UFRJ 13199, 4 ex., 24.4–46.7 mm SL; Rio Humboldt, Osvaldo Amaral, 26°23′21″ S 49°15′12″ W, about 90 m; C. R. M. Feltrin, 31 August 2022. UFRJ 13206, 2 ex., 50.0–75.2 mm SL; Rio Isabel, tributary of Rio Novo, 26°28′45″ S 49°18′16″ W, about 165 m asl; C. R. M. Feltrin, 30 August 2022. Jaraguá do Sul Municipality: CICCAA 07551; 2 ex., 36.0–46.3 mm SL; Rio Jaraguá, about 1 km SE from the village of Garibaldi, 26°31′34″ S 49°12′49″ W, about 75 m asl; C. R. M. Feltrin, 15 April 2022. São Bento do Sul Municipality: MHNCI 11949, 9 ex., 31.1–77.5 mm SL; Rio Vermelho, a tributary of Rio Humboldt, 49°19′12″ W 26°18′35″ S, about 730 m asl; V. Abilhoa, L.F. Duboc and P. Pinheiro, 8 August 2006.

Diagnosis. *Cambeva ventropapillata* is distinguished from all congeners, except *C. papillifera* (Wosiacki & Garavello, 2004), by having broad laminar, ribbon-shaped nasal barbels (vs. narrow, wire-shaped), maxillary and rictal barbels broad at their basal portion, abruptly narrowing distally (vs. not distinctively widened at the proximal portion, gradually narrowing distally), and large skin papillae on the ventral surface of the head (vs. papillae minute or rudimentary). *Cambeva ventropapillata* differs from *C. papillifera* by having longer maxillary and rictal barbels, their tips posteriorly reaching the anterior region of the interopercular patch of odontodes (vs. reaching area about midway between barbel base and interopercular patch of odontodes), mouth subterminal (vs. ventral), and the anal-fin origin at a vertical through the posterior portion of the dorsal-fin base (vs. through the middle of the dorsal-fin base).

Description. General morphology: Morphometric data are presented in Table 3. Body slender to moderately deep, subcylindrical on anterior region, compressed on posterior region. Greatest body depth in area immediately anterior to pelvic-fin base. Dorsal

profile slightly convex between snout and dorsal-fin base end, nearly straight on caudal peduncle; ventral profile convex on head, approximately straight on trunk. Anus and urogenital papilla opening at vertical through area just posterior to dorsal-fin origin. Head sub-trapezoidal, with anterior profile of snout slightly convex in dorsal view. Eye small, dorsally positioned on head, nearer snout tip than posterior margin of opercle. Distance between anterior and posterior nostrils about half distance between posterior nostril and orbital rim. Barbels broad, short, nasal barbel ribbon-shaped, often with waved margin, maxillary and rictal barbels abruptly narrowing distally. Tip of nasal barbel posteriorly reaching posterior margin of orbit or area immediately posterior to it, tip of maxillary and rictal barbels reaching anterior region of interopercular patch of odontodes. Mouth subterminal. Lateral fleshy lobe of the mouth moderate in size, its largest length about one-third of lower jaw length excluding lobes; ventral surface of lobe flat. Jaw teeth irregularly arranged, more external teeth longer, tip pointed to slightly rounded, 44–48 on premaxilla, 39–48 on dentary. Well-developed skin papillae on ventral surface of head, diameter of larger papilla about one-fifth of orbital diameter. Skin papillae extending over ventral and dorsal surfaces of snout and lateral lobe of mouth. Branchial membrane attached to isthmus only at its anterior-most point, in ventral midline.

Dorsal and anal fins subtriangular, margins about straight, dorsal fin moderately deep, longest ray longer than fin base. Total dorsal-fin rays 12–13 (iii–iv + II + 7), total anal-fin rays 10 (iii + II + 5). Anal-fin origin at vertical through posterior portion to dorsal-fin base, between bases of 5th and 6th bifid rays. Dorsal-fin origin at vertical through centrum of 20th or 21st vertebra; anal-fin origin at vertical through centrum of 25th or 26th vertebra. Pectoral fin subtriangular in dorsal view, margins rounded. First pectoral-fin ray shorter than second ray, not forming terminal filament. Total pectoral-fin rays 7 (I + 6). Pelvic fin subtruncate, its posterior extremity in vertical at dorsal-fin origin. Pelvic-fin bases medially separated by minute interspace. Total pelvic-fin rays 5 (I + 4). Caudal fin subtruncate, posterior corners rounded. Total principal caudal-fin rays 13 (I + 11 + I), total dorsal procurrent rays 17–20 (xvi–xix + I), total ventral procurrent rays 10–13 (ix–xii + I).

Laterosensory system: Supraorbital, posterior section of infraorbital canal and postorbital canal continuous. Supraorbital sensory canal pores 3: s1, adjacent to medial margin of anterior nostril; s3, adjacent and just posterior to medial margin of posterior nostril; s6, in transverse line through posterior half of orbit; pore s6 slightly nearer orbit than its paired s6 homologous pore. Anterior infraorbital sensory canal usually closed with pores 2: i1, at transverse line through anterior nostril, and i3, at transverse line just anterior to posterior nostril; sometimes canal opened. Posterior infraorbital sensory canal pores 2: pore i10, adjacent to ventral margin of orbit, and pore i11, posterior to orbit. Postorbital canal pores 2: po1, at vertical through posterior portion of interopercular patch of odontodes, and po2, at vertical through posterior portion of opercular patch of odontodes. Lateral line pores 2; posterior-most pore at vertical just posterior to pectoral-fin base.

Osteology: Mesethmoid thin, anterior margin straight to slightly convex. Mesethmoid cornu narrow, tip rounded. Lateral margin of lateral ethmoid without projections. Antorbital thin, sub-elliptical, about half length of premaxilla. Sesamoid supraorbital slender, flat, without lateral projections, its length about two and half times antorbital length. Premaxilla sub-trapezoidal in dorsal view, laterally narrowing, approximately equal to maxilla in length. Maxilla slightly curved. Autopalatine sub-rectangular in dorsal view when excluding its postero-lateral process, its largest width about half of its length when excluding anterior cartilage; medial margin, with deep concavity in middle portion. Autopalatine posterolateral process well-developed, its length about two-thirds of autopalatine length. Metapterygoid thin, longer than deep. Quadrate slender, dorsal process with constricted base, dorsoposterior margin in contact with hyomandibula outgrowth. Hyomandibula long, with well-developed anterior outgrowth; dorsal margin of hyomandibula outgrowth without pronounced concavities. Opercle long, longer than interopercle; opercular odontode patch robust, its width about three-fourths of dorsal hyomandibula articular facet. Opercular odontodes 13–24, straight and pointed, irregularly arranged. Dorsal process of

opercle short, nearly straight; opercular articular facet for hyomandibula with rounded flap, articular facet for preopercle slightly smaller than articular facet for hyomandibula, rounded. Interopercle moderate in length, about equal to hyomandibula outgrow horizontal length, with about straight anterior margin and prominent anterior process on its dorsal limit. Interopercular odontodes 16–24, nearly straight, pointed, longer odontodes about as long as larger opercular odontodes, arranged in irregular longitudinal rows. Preopercle compact, with minute ventral projection. Parurohyal robust, lateral process triangular, posterior margin straight. Parurohyal head well-developed, with prominent anterolateral paired process. Middle parurohyal foramen large, elliptical. Posterior process of parurohyal moderately long, about half distance between anterior margin of parurohyal and anterior insertion of posterior process. Branchiostegal rays 8 or 9. Vertebrae 39–41. Ribs 13 or 14. Two dorsal hypural plates corresponding to hypurals 3 + 4 + 5; single ventral hypural plate corresponding to hypurals 1 + 2 and parhypural.

Colouration in alcohol: Head and trunk light grey to brown, slightly darker on dorsum, humeral region and area around opercular and interopercular patches of odontodes. Venter white. Fins hyaline with basal portion dark grey to brown. In specimens below about 45 mm SL, dorsal part of flank and dorsum with faint grey dots.

Etymology. From the Latin, *ventro* (venter) and *papillata* (with papillae), an allusion to the well-developed papillae on the ventral surface of the head.

Distribution and habitat notes. Cambeva ventropapillata is known from the Rio Itapocu basin, occurring in the upper section of the western and south-western part of the basin (Figure 3), in altitudes between about 35 and 165 m asl. Habitats were streams with moderate current, with deepest areas reaching about 0.8 m. Specimens of *Cambeva ventropapillata* were found among small and medium pebbles (grain sizes ranging from 0.01 to 0.5 m). Larger specimens of the type series were found in association with marginal plants and ravines, in a mixture of pebbles, clayey soil, macrophytes and margin grasses. Larger specimens also showed preference for larger pebbles, when compared to small specimens. Specimens were also often found at the middle of the river channel. In the Rio Treze de Maio, the water was cloudy, indicating a high degree of pollution. In this area, the riparian forests were preserved at some points, anthropized in others, and absent in certain places. Downstream of the type locality, the water was being used for the irrigation of small and medium-sized plantations. Even considering that the basin is under different environmental impacts, the species was not rare, being easily recorded in different areas of the basin.

Remarks. Cambeva ventropapillata was formerly misidentified as *T. nigricans* by de Pinna (1992), based on four specimens deposited in the Museu de Ciências e Tecnologia, Pontifícia Universidade Católica do Rio Grande do Sul, Porto Alegre, Brazil (MCP 10649), which were examined by one of us (WJEMC, 1992). See Costa et al. (2020b) for a historical review about equivocal localities and misidentification of *T. nigricans*.

3.2.2. *Cambeva* Gama-Clade

Cambeva biseriata sp. nov.

LSID:urn:lsid:zoobank.org:act:3524D6F0-BD72-49EC-B6F9-AEB7FA6D03C6

Figure 7F, Figure 8F, Figure 9F, Figure 14 and Table 4, respectively.

Holotype. UFRJ 13265, 70.8 mm SL; Brazil: Santa Catarina State: Joinville Municipality: Rio Piraí, Rio Itapocu basin, Vila Nova, 26°17′34″ S 48°57′51″ W, about 30 m asl; C. R. M. Feltrin, 14 August 2020.

Paratypes. All from Brazil: Santa Catarina State: Rio Itapocu basin. Joinville Municipality. UFRJ 13263, 3 ex. (C&S), 42.5–55.4 mm SL; UFRJ 13264, 2 ex., 39.5–55.4 mm SL; collected with holotype. CICCAA 07548, 3 ex., 34.9–70.8 mm SL; UFRJ 11320, 3 ex. (C&S), 51.7–68.1 mm SL; Rio Mutucas, Rio Piraí drainage, 26°14′38″ S 48°56′48″ W, about 95 m asl; R. Dalcin, 23 January 2016. UFRJ 12305, 8, 61.3–86.4 mm SL; Rio Tateto, 26°15′50″ S 48°58′51″ W, about 90 m asl; R. Dalcin, 18 April 2014. UFRJ 12878, 4, 67.3–75.7 mm SL; same locality and collector as UFRJ 12305, 15 April 2014. UFRJ 12979, 6, 46.1–74.5 mm SL; Jaraguá do Sul Municipality: Rio Itapocuzinho, 26°19′18″ S 49°08′44″ W, about 290 m asl;

R. Dalcin, 7 March 2021. Guaramirim Municipality: UFRJ 13266, 6 ex., 36.3–57.1 mm SL; stream tributary to Rio Piraí, Bruderthal, near Pedra Sapo, 26°25′40″ S 48°59′07″ W, about 40 m asl; C. R. M. Feltrin, 6 November 2020. UFRJ 12872, 2 ex. (DNA), 40.6–59.2 mm SL; same locality as UFRJ 13266; C. R. M. Feltrin, 15 April 2022.

Figure 14. *Cambeva biseriata* sp. nov., UFRJ 13265, holotype, 70.8 mm SL: (**A**) lateral, (**B**) dorsal, and (**C**) ventral views.

Table 4. Morphometric data of *Cambeva biseriata* sp. nov.

	Holotype	**Paratypes (n = 10)**
Standard length (SL)	70.8	42.5–74.5
Percentage of standard length		
Body depth	15.4	13.5–17.0
Caudal peduncle depth	12.4	11.3–14.4
Body width	10.9	10.8–13.0
Caudal peduncle width	3.5	3.1–4.2
Pre-dorsal length	61.7	61.1–64.3
Pre-pelvic length	54.7	55.5–62.6
Dorsal-fin base length	10.3	10.9–12.5
Anal-fin base length	9.1	8.1–10.9
Caudal-fin length	15.8	15.2–17.9
Pectoral-fin length	12.3	11.7–13.6
Pelvic-fin length	9.6	8.5–10.5
Head length	20.0	19.4–22.6
Percentage of head length		
Head depth	45.6	44.7–52.2
Head width	80.8	73.9–85.2
Snout length	41.7	40.8–46.3
Interorbital width	22.6	21.9–26.0
Preorbital length	14.3	12.4–15.8
Eye diameter	10.7	9.6–12.2

Diagnosis. Cambeva biseriata is distinguished from all other congeners of the *C. balios-C. tropeira* clade by having a unique colour pattern, consisting of two longitudinal rows of small brown rounded spots, one along the lateral midline of body and the other on the dorsal part of flank, overlapped by minute pale brown dots scattered over the entire flank and dorsum (vs. never a similar colour pattern), jaw teeth incisiform (vs. pointed in *C. balios*, *C. duplimaculata*, *C. longipalata*, *C. notabilis*, *C. tropeira*, and *C. urubici*, pointed to sub-incisiform, with rounded extremity, in *C. diffusa* and *C. pericoh*), and more dorsal procurrent rays in the caudal fin (18 or 19, vs. 12–17). *Cambeva biseriata* also differs from *C. balios*, *C. diffusa*, *C. duplimaculata*, *C. longipalata*, *C. notabilis*, *C. pericoh*, *C. tropeira* and *C. urubici* by having a large lateral fleshy lobe of the mouth, its largest length occupying about three-fourths of the lower jaw length excluding lobes (vs. about one fourth to one third), and from *C. duplimaculata*, *C. longipalata*, *C. notabilis*, *C. tropeira* and *C. urubici* by the absence of the anterior section of the infraorbital canal absent (vs. presence). *Cambeva biseriata* is also distinguished from all congeners, except *C. longipalata*, by having a long postero-lateral process of the autopalatine, its length about equal to the autopalatine length (vs. about two thirds). *Cambeva biseriata* is further distinguished from *C. longipalata* by having more ventral procurrent rays in the caudal fin (13–15 vs. 10–12) and fewer vertebrae (37–39 vs. 41–42).

Description. General morphology: Morphometric data are presented in Table 4. Body moderately slender, subcylindrical on anterior region, compressed on posterior region. Greatest body depth in area just anterior to pelvic-fin base. Dorsal and ventral profiles slightly convex between snout and anterior portion of caudal peduncle, nearly straight on caudal peduncle. Anus and urogenital papilla opening at vertical just posterior to dorsal-fin origin. Head sub-trapezoidal in dorsal view, with anterior profile of snout nearly straight. Eye small, dorsally positioned on head, nearer snout tip than posterior margin of opercle. Distance between anterior and posterior nostrils about one-third distance between posterior nostril and orbital rim. Barbels moderate in length, tip of nasal barbel posteriorly reaching area between orbit and preopercle, tip of maxillary and rictal barbels reaching interopercular patch of odontodes, or sometimes rictal barbel reaching area just anterior to interopercular patch of odontodes. Mouth subterminal. Lateral fleshy lobe of the mouth large, its largest length about three-fourths of lower jaw length excluding lobes; ventral surface of lobe slightly concave. Jaw teeth incisiform, irregularly arranged, 48–50 on premaxilla, 47–62 on dentary. Minute skin papillae on ventral surface of head, conspicuous only on area just anterior to branchiostegal region. Branchial membrane attached to isthmus only at its anterior-most point, in ventral midline.

Dorsal and anal fins subtriangular, anterior margin about straight, posterior margin weakly convex, longest ray about equal fin base in length. Total dorsal-fin rays 12 (iii + II + 7), total anal-fin rays 10 (iii + II + 5). Anal-fin origin at vertical through middle portion of dorsal-fin base, at vertical of 4th bifid ray. Dorsal-fin origin at vertical through centrum of 20th or 21st vertebra; anal-fin origin at vertical through centrum of 24th vertebra. Pectoral fin subtriangular in dorsal view, posterior margin convex. First pectoral-fin ray about equal second ray in length, not forming terminal filament. Total pectoral-fin rays 7 (I + 6). Pelvic fin rounded, its posterior extremity at vertical through dorsal-fin origin. Pelvic-fin bases medially in close proximity, almost in contact. Total pelvic-fin rays 5 (I + 4). Caudal fin truncate. Total principal caudal-fin rays 13 (I + 11 + I), total dorsal procurrent rays 17–19 (xvi–xviii + I), total ventral procurrent rays 13–15 (xii–xiv + I).

Laterosensory system: Supraorbital, posterior section of infraorbital canal and postorbital canal continuous. Supraorbital sensory canal pores 3: s1, adjacent to medial margin of anterior nostril; s3, adjacent and just posterior to medial margin of posterior nostril; s6, in transverse line through posterior half of orbit; pore s6 slightly nearer orbit than its paired s6 homologous pore. Anterior infraorbital sensory canal absent. Posterior infraorbital sensory canal pores 2: pore i10, adjacent to ventral margin of orbit, and pore i11, posterior to orbit. Postorbital canal pores 2: po1, at vertical through posterior portion of interopercular patch of odontodes, and po2, at vertical through posterior portion of opercular patch of

odontodes. Lateral line pores 2; posterior-most pore at vertical just posterior to pectoral-fin base.

Osteology: Mesethmoid thin, anterior margin straight to slightly convex, main axis tapering posteriorly. Mesethmoid cornu narrow, tip rounded. Lateral surface of lateral ethmoid with pronounced projection posterior to articular connection to autopalatine. Antorbital thin, sub-elliptical, small, about one-fourth of half length of sesamoid supraorbital. Sesamoid supraorbital relatively slender, flat, with small postero-lateral projection, its length about equal autopalatine length. Premaxilla sub-trapezoidal in dorsal view, laterally narrowing, slightly longer than maxilla. Maxilla gently curved. Autopalatine sub-rectangular in dorsal view when excluding its postero-lateral process, its largest width about two three-fourths its length excluding anterior cartilage; medial margin slightly sinuous. Autopalatine posterolateral process long, its length about equal to autopalatine length. Metapterygoid thin, longer than deep. Quadrate slender, dorsal process with constricted base, dorsoposterior margin in contact with hyomandibula outgrowth. Hyomandibula long, with well-developed anterior outgrowth; dorsal margin of hyomandibula outgrowth with shallow concavity. Opercle moderately long, longer than interopercle; opercular odontode patch robust, its width about slightly smaller than dorsal hyomandibula articular facet. Opercular odontodes 15, irregularly arranged, narrow, largest odontodes slightly curved. Dorsal process of opercle short, extremity rounded. Opercular articular facet for hyomandibula with rounded flap, articular facet for preopercle indistinct. Interopercle relatively short, its longitudinal length smaller than hyomandibula outgrow horizontal length; anterior margin of interopercle about straight. Interopercular odontodes 23, nearly straight to slightly curved, pointed, arranged in irregular longitudinal rows, largest odontodes slightly smaller than largest opercular odontodes, irregularly arranged. Preopercle compact, with minute ventral projection. Parurohyal robust, lateral process slightly curved, with subtruncate distal extremity. Parurohyal head well-developed, with prominent antero-lateral paired process. Middle parurohyal small, elliptical. Posterior process of parurohyal moderately long, about three-fifths distance between anterior margin of parurohyal and anterior insertion of posterior process. Branchiostegal rays 8 or 9. Vertebrae 37–39. Ribs 13. Two dorsal hypural plates corresponding to hypurals 3 + 4 + 5; single ventral hypural plate corresponding to hypurals 1 + 2 and parhypural.

Colouration in alcohol: Flank and dorsum pale yellow; longitudinal row of small brown rounded spots along lateral midline of body, between humeral region and caudal peduncle, spot diameter about equal opercular patch of odontodes or slightly smaller; longitudinal row of dark brown rounded spots on dorsal part of flank, between nape region and caudal peduncle, spot diameter about four times opercular patch of odontodes or slightly larger; minute pale brown dots scattered over whole flank and dorsum. Dorsal and lateral portion of head pale yellow with dark brown blotches. Venter and ventral surface of head white. Barbels pale yellow with brown margins on dorsal surface, light grey to white in ventral surface. Fins hyaline with brown blotches on basal portion.

Etymology. From de Latin *biseriata* (with two series), referring to the two longitudinal series of brown spots on the flank that is diagnostic for this new species.

Distribution and ecological notes. *Cambeva biseriata* is only known from the northern portion of the Rio Itapocu basin (Figure 3), in altitudes between about 30 and 290 m asl. *Cambeva biseriata* occurs in lotic/semi-lotic environments, closely associated with stony substrate, with granulometries ranging from 0.01 to 0.6 m, and low depths, between 0.5 and 0.8 m. The channel of the Rio Piraí, in Vila Nova, Joinville, has an average width of 21 m, and depths ranging from 5 cm to more than 2 m. The tributary creek of the Rio Piraí has widths that vary between 1.5 and 8.5 m, with depths not exceeding 1 m, prevailing small and medium rolled pebbles. Like other congeners, smaller individuals were distributed preferably in shallow places, with fine gravel and small pebbles about 0.01 to 0.20 in diameter, sometimes associated with marginal vegetation and/or leaf litter deposits. Larger specimens were found below large pebbles, about 0.4 m or more in diameter. In the tributary creek of the Rio Piraí, in Bruderthal, this species is still abundant

in places without human intervention, mainly in those with well-preserved riparian forests. Irrigated rice monoculture activities represent, at the sub-basin level of the Rio Piraí, the main threat to *C. biseriata*. Such activity promotes the diversion of natural waters from rivers and streams, in addition to an immeasurable load of silting up of clay fines, agricultural defensives, deconfiguration of streams or even total suppression.

3.3. Key to Identification of Species of Cambeva from GBIA

1A. Anterior infraorbital canal present. → 2

1B. Anterior infraorbital canal absent. → 3

2A. Anal-fin origin at vertical through posterior portion of dorsal-fin base, at vertical of 6th bifid ray; posterior margin of caudal fin straight; papilla urogenital at vertical just posterior to dorsal-fin origin; 17–19 dorsal procurrent caudal-fin rays. → *Cambeva biseriata*

2B. Anal-fin origin at vertical through middle portion to dorsal-fin base, at vertical of 4th bifid ray; posterior margin of caudal fin slightly convex; papilla urogenital at vertical through middle of dorsal-fin base; 21–22 dorsal procurrent caudal-fin rays. → *Cambeva* cf. *botuvera*

3A. Nasal barbel broad laminar, ribbon-shaped; flank and dorsum predominantly dark grey to dark brown, never with yellow marks; odontodes always with pointed extremity. → *Cambeva ventropapillata*

3B. Nasal barbel narrow, wire-shaped; flank and dorsum predominantly dark grey to black contrasting with bright yellow marks at least in specimens above 40 mm SL; odontodes with rounded extremity at least on internal-most series of interopercle in specimens above about 60 mm SL. → 4

4A. Tip of rictal barbel posteriorly reaching anterior margin of orbit or area anterior to it; maxillary and rictal barbels not reaching interopercular patch of odontodes; longest dorsal-fin ray shorter than dorsal-fin base; pectoral fin rounded in dorsal view; pelvic fin rounded, its posterior extremity reaching vertical anterior to dorsal-fin origin; 16 or 17 dorsal procurrent caudal-fin rays; 11 or 12 ventral procurrent caudal-fin rays. → *Cambeva chrysornata*

4B. Tip of rictal barbel posteriorly reaching area posterior to orbit; maxillary and rictal barbels posteriorly reaching interopercular patch of odontodes; longest dorsal-fin ray longer than dorsal-fin base; pectoral fin subtriangular in dorsal view; pelvic fin rounded, its posterior extremity reaching a vertical anterior to the dorsal-fin origin; pelvic fin truncate, its posterior extremity reaching vertical through anterior half of dorsal-fin base; 20 or 21 dorsal procurrent caudal-fin rays; 13 or 14 ventral procurrent caudal-fin rays. → 5

5A. Jaw teeth irregularly arranged, with pointed to rounded tip; (vs. teeth, arranged in), more 18–20 opercular odontodes. → *Cambeva cubataonis*

5B. Jaw teeth regularly arranged in three rows, with truncate to slightly bilobed tip; 13–16 opercular odontodes. → *Cambeva guaratuba*

4. Discussion

4.1. The Use of Morphological Characters to Diagnose Species of Cambeva

Among the most widely used morphological characters to diagnose the species of *Cambeva* are the number of pectoral-fin rays and the colour pattern. The combination of these two characters has been used in diagnoses of the vast majority of descriptions of the new species of *Cambeva*, with one or both of them being the first step indicated in diagnoses to distinguish the new taxon from congeners (e.g., [11,19,57–59]). Consequently, it is understandable that attempts to identify species in regional ichthyological inventories primarily take these two groups of characters into account. However, in GBIA, where all species have the same number of pectoral-fin rays and there is a marked degree of chromatic polymorphism in *C.* cf. *botuvera*, these characters should not be used alone for distinguishing species. Thus, the use of a limited set of morphological characters may lead to misidentifications and a consequent underestimation of the number of species in a given area.

The use of osteological characters has shown to be revealing to distinguish supposedly closely related species, with the morphology of the parurohyal and bones of the

mesethmoidal and check regions being particularly informative for diagnosing species and for supporting hypotheses of species relationships [4,6,7,10,11,14,19,57–60]. Although not being possible to check bone morphology variation in large intraspecific specimen samples and osteological data are still unavailable for some valid species, osteological characters may be more effective for distinguishing taxa than diagnostic characters taken from the external morphology (see above morphological characters distinguishing *C.* cf. *botuvera* and *C. cubataonis*). Furthermore, morphological characters are important to validate the results of coalescent-based species delimitation [61,62]. In the case of trichomycterines, osteological characters associated with slight variation in characters of the external morphology may highly corroborate molecular species delimitation [16]. In addition, osteological characters may have a crucial role in clarifying the taxonomical status of trichomycterine lineages with similar external morphology [12] and are useful to diagnose trichomycterine clades previously supported only by molecular data [3]. Therefore, we strongly recommend the use of comparative osteology in studies involving taxonomical decisions at the species level in *Cambeva* and other trichomycterines.

4.2. The Use of Single-Locus Coalescent Approaches to Delimitate Trichomycterine Species

In the last 15 years, species delimitation became one of the most frequent themes in scientific journals of biological sciences. Among the most popular methods for species delimitation are the single-locus coalescent approaches, such as the Generalised Mixed Yule Coalescent (GMYC) method [63,64] and the Poisson tree processes (PTP) model [61], which may be more efficient to delimitate species than the equally popular distance methods [65]. These coalescent-based methods use algorithms that work by detecting gaps in gene trees (i.e., branch length gaps in time-calibrated ultrametric tree for GMYC and number variation gaps of nucleotide substitutions in tree nodes for PTP) to define the transitions between inter and intra-specific processes (e.g., [64]). Since gaps yield the main signal to detect speciation events, making these methods highly sensitive to gaps artificially generated by taxon undersampling, it is necessary to use multiple sequenced individuals representing all populations of taxa forming a monophyletic group [64]. Therefore, random species samples belonging to different clades containing incomplete taxon samplings may produce equivocal or incongruent results, tending to lose accuracy when groups of distant taxa or different groups are placed in the same analysis.

Donin et al. [30] performed GMYC and PTB analyses with different configurations, using a 597 bp COX1 data set for haplotypes representing 22 morphotypes, including 20 nominal species and two unidentified species. Instead of focusing on specific monophyletic groups, the taxon sample was mainly directed to species collected in the coastal river basins of south-eastern and southern Brazil. Consequently, the taxon sampling comprised representatives of the three main intrageneric clades (i.e., alpha, beta and gama-clades as described in results above), making taxon sample paraphyletic by not representing most lineages of the alpha and beta-clades that are endemic to areas out of the coastal basins (i.e., several species endemic to the Iguaçu and Uruguai river basins). These analyses generated discrepant species delimitation results, recognising since only five species to over 100 species in *Cambeva*, probably as a result of incomplete taxon sampling for each of the different clades analysed.

In GBIA, Donin et al. [30] identified only two morphotypes, *C. barbosae* and *C. cubataonis*, but the latter morphotype independently appeared in four different species delimited in the GMYC single-threshold model (combination 4), which was the single delimitation illustrated in the main text of the paper [30] (Figure 11 in Ref. [30]). Instead of admitting the possibility of existing four distinct species, this supposed discordance between morphological data supporting recognition of morphotypes and the results of the molecular species delimitation was interpreted by Donin et al. [30] as a failure of single-locus data in delimiting species of *Cambeva*. One of the species from GBIA delimited by Donin et al. [30] (Figure 11 in Ref. [30]) included a sequence of the specimen identified as *C. cubataonis* by Katz et al. [21] and specimens identified by the authors as *C. barbosae* morphotypes, thus

constituting the same polymorphic taxon here identified as *C.* cf. *botuvera*, geographically widespread species closely related to *C. barbosae* (Figure 1). The three other delimited species comprised a monophyletic group, in which a species with two haplotypes from the Baía de Guaratuba system was sister to a clade comprising two species, one represented by a single haplotype from the Baía de Paranaguá system, an area not included in our inventories, and another with haplotypes from the Rio Cubatão do Norte basin and from the Baía de Babitonga system.

Checking external morphological features of specimens illustrated in Donin et al. [30] (Figure 6 in Ref. [30]), including barbel and fin morphology and colour pattern, it is possible to unambiguously identify the species from the Baía de Guaratuba system [30] (Figure 6A,B in Ref. [30]) as the species here described as *C. guaratuba* and the species from the Baía de Babitonga system [30] (Figure 6C–E in Ref. [30]) as the species here described as *C. chrysornata*. These data indicate that this species delimitation analysis recognised *C. guaratuba* as a distinct species, but it was not able to differentiate *C. chrysornata* and *C. cubataonis*, which are herein supported as sister taxa, but distinguished from each other by several morphological characters (see diagnoses above). Therefore, we conclude that the COX1 coalescent-based analysis by Donin et al. [30] is not in discordance with morphological data but had no resolution to delimit *C. chrysornata* and *C. cubataonis*, probably by the taxon sampling problems above described and the use of only a short segment of COX1. It is remarkable that in a former study using both COX1 and CYTB [17] (Supplementary File S4 in Ref. [17]), haplotypes of *C. chrysornata* and *C. cubataonis* appeared as well-structured sister exclusive lineages, thus corroborating our results.

Appendix A

Terminal taxa for molecular phylogeny and respective GenBank accession numbers.

	COX1	CYTB	RAG2
Nematogenys inermis	KY857952	-	KY858182
Copionodon pecten	KY857929	-	KY858169
Trichogenes longipinnis	MK123682	MK123704	MF431117
Microcambeva ribeirae	MN385807	OK334290	MN385832
Listrura tetraradiata	MN385804	JQ231088	MN385826.1
Eremophilus mutisii	KY857931	-	KY858171
Ituglanis boitata	MK123684	MK123706	MK123758
Bullockia maldonadoi	KY857926	FJ772237	KY858166
Scleronema minutum	MK123685	MK123707	MK123759.1
Scleronema auromaculatum	OM037445	OM037134	OM037136
Trichomycterus itatiayae	MW671552	MW679291	KY858198
Trichomyctetrus nigricans	MN813005	MK123723	MK123765
Cambeva variegata	KY857991	OQ110805	KY858211
Cambeva cf. *botuvera*	MK123689	MK123713	MN385820
Cambeva zonata	KY857986	KY858053	-
Cambeva brachykechenos	MN995669	MN995758	-
Cambeva diatropoporos	KY857996	KY858065	KY858213
Cambeva davisi	KR140345	MK123714	MK123762
Cambeva stawiarski	MN995720	MN995779	-
Cambeva perkos	KY857981	KY858050	KY858213
Cambeva poikilos	KY857995	KY858064	-
Cambeva guaraquessaba	MN995662	MN995749	-
Cambeva naipi	MN995699	MN995771	-
Cambeva taroba	MN995708	MN995757	-
Cambeva tupinamba	MN995656	MN995751	-
Cambeva tropeira	MN995674	MN995752	-
Cambeva grisea	MN995671	MN995760	-
Cambeva imaruhy	MN995700	MN995766	-
Cambeva orbitofrontalis	MN995703	MN995764	-
Cambeva cubataonis	OQ095914	OQ110814	OQ110815
Cambeva iheringi	GU701893	KY858074	KY858223
Cambeva cf. *diabola*	JN989258	OQ110812	-
Cambeva balios	MN995682	MN995755	-
Cambeva castroi	-	MK123712	OQ110816
Cambeva biseriata	-	OQ110806	OQ110817
Cambeava ventropapillata	-	OQ110807	OQ110818
Cambeva barbosae	-	OQ110808	-
Cambeva botuvera	-	OQ110809	-
Cambeva chrysornata	MN995726	OQ110810	OQ110819
Cambeva pascuali	MF034463	OQ110811	OQ110820
Cambeva guareiensis	-	OQ110813	OQ110821
Cambeva guaratuba	MN995721	MN995792	-

Appendix B

Best-Fitting Partition Schemes and Evolutive Models		
Partition	Base Pairs	Evolutive Model
COX1 1st	174	TRN + I + G
COX1 2nd	174	F81 + I
COX1 3rd	174	TIM + G
CYTB 1st	331	TVMEF + I + G
CYTB 2nd	331	HKY + I
CYTB 3rd	331	TRN + I + G
RAG2 1st	263	TVMEF + I
RAG2 2nd	263	TVM + G
RAG2 3rd	262	HKY + I

References

1. Albert, J.S.; Tagliacollo, V.A.; Dagosta, F.C.P. Diversification of Neotropical freshwater fishes. *Ann. Rev. Ecol. Evol. Syst.* **2020**, *51*, 27–53. [CrossRef]
2. Fricke, R.; Eschmeyer, W.N.; Van der Laan, R. Eschmeyer's Catalog of Fishes: Genera, Species, References. 2022. Available online: http://researcharchive.calacademy.org/research/ichthyology/catalog/fishcatmain.asp (accessed on 3 December 2022).
3. Costa, W.J.E.M. Comparative osteology, phylogeny and classification of the eastern South American catfish genus *Trichomycterus* (Siluriformes: Trichomycteridae). *Taxonomy* **2021**, *1*, 160–191. [CrossRef]
4. Costa, W.J.E.M.; Feltrin, C.R.M.; Katz, A.M. A new species from subtropical Brazil and evidence of multiple pelvic fin losses in catfishes of the genus *Cambeva* (Siluriformes, Trichomycteridae). *Zoosyst. Evol.* **2020**, *96*, 715–722. [CrossRef]
5. Costa, W.J.E.M.; Mattos, J.L.O.; Amorim, P.F.; Vilardo, P.J.; Katz, A.M. Relationships of a new species support multiple origin of melanism in *Trichomycterus* from the Atlantic Forest of south-eastern Brazil (Siluriformes: Trichomycteridae). *Zool. Anz.* **2020**, *288*, 74–83. [CrossRef]
6. Costa, W.J.E.M.; Feltrin, C.R.M.; Katz, A.M. Filling distribution gaps: Two new species of the catfish genus *Cambeva* from southern Brazilian Atlantic Forest (Siluriformes: Trichomycteridae). *Zoosyst. Evol.* **2021**, *97*, 147–159. [CrossRef]
7. Costa, W.J.E.M.; Feltrin, C.R.M.; Katz, A.M. Field inventory reveals high diversity of new species of mountain catfishes, genus *Cambeva* (Siluriformes: Trichomycteridae), in south-eastern Serra Geral, southern Brazil. *Zoosystema* **2021**, *43*, 659–690. [CrossRef]
8. Costa, W.J.E.M.; Mattos, J.L.O.; Katz, A.M. Two new catfish species from central Brazil comprising a new clade supported by molecular phylogeny and comparative osteology (Siluriformes: Trichomycteridae). *Zool. Anz.* **2021**, *293*, 124–137. [CrossRef]
9. Costa, W.J.E.M.; Abilhoa, V.; Dalcin, R.H.; Katz, A.M. A new catfish species of the genus *Cambeva* (Siluriformes: Trichomycteridae) from the Rio Iguaçu drainage, southern Brazil, with a remarkable unique colour pattern. *J. Fish Biol.* **2022**, *101*, 69–76. [CrossRef]
10. Costa, W.J.E.M.; Feltrin, C.R.M.; Katz, A.M. Two new remarkable and endangered catfish species of the genus *Cambeva* (Siluriformes, Trichomycteridae) from southern Brazil. *Eur. J. Taxonomy* **2022**, *794*, 140–155. [CrossRef]
11. Costa, W.J.E.M.; Feltrin, C.R.M.; Katz, A.M. An endangered new catfish species of the genus *Cambeva* (*Cambeva gamabelardense* n. sp.) (Siluriformes, Trichomycteridae) from the Rio Chapecó drainage, southern Brazil. *Anim. Biodivers. Conserv.* **2022**, *45*, 123–129. [CrossRef]
12. Costa, W.J.E.M.; Mattos, J.L.; Vilardo, P.J.; Amorim, P.F.; Katz, A.M. Perils of underestimating species diversity: Revisiting systematics of *Psammocambeva* catfishes (Siluriformes: Trichomycteridae) from the Rio Paraíba do Sul Basin, south-eastern Brazil. *Taxonomy* **2022**, *2*, 491–523. [CrossRef]
13. Costa, W.J.E.M.; Sampaio, W.M.S.; Giongo, P.; de Almeida, F.B.; Azevedo-Santos, V.M.; Katz, A.M. An enigmatic interstitial trichomycterine catfish from south-eastern Brazil found at about 1000 km away from its sister group (Siluriformes: Trichomycteridae). *Zool. Anz.* **2022**, *297*, 85–96. [CrossRef]
14. Katz, A.M.; Costa, W.J.E.M. A new species of the catfish genus *Cambeva* from the Paranapanema river drainage, southeastern Brazil (Siluriformes: Trichomycteridae). *Trop. Zool.* **2020**, *33*, 2–13. [CrossRef]
15. Costa, W.J.E.M.; Katz, A.M. A new catfish of the genus *Trichomycterus* from the Rio Paraíba do Sul Basin, south-eastern Brazil, a supposedly migrating species (Siluriformes, Trichomycteridae). *Zoosyst. Evol.* **2021**, *98*, 13–21. [CrossRef]
16. Costa, W.J.E.M.; Katz, A.M. Integrative taxonomy supports high species diversity of south-eastern Brazilian mountain catfishes of the *T. reinhardti* group (Siluriformes: Trichomycteridae). *Syst. Biodivers.* **2021**, *19*, 601–621. [CrossRef]
17. Donin, L.M.; Ferrer, J.; Carvalho, T.P. Taxonomical study of *Trichomycterus* (Siluriformes: Trichomycteridae) from the Ribeira de Iguape River basin reveals a new species recorded in the early 20th century. *J. Fish Biol.* **2020**, *96*, 886–904. [CrossRef] [PubMed]
18. Vilardo, P.J.; Katz, A.M.; Costa, W.J.E.M. Relationships and description of a new species of *Trichomycterus* (Siluriformes: Trichomycteridae) from the Rio Paraíba do Sul basin, south-eastern Brazil. *Zool. Stud.* **2020**, *59*, 53. [CrossRef]
19. Dos Reis, R.B.; Ferrer, J.; da Graça, W.J. A new species of *Cambeva* (Siluriformes, Trichomycteridae) from the Rio Iguaçu basin, Paraná state, Brazil and redescription of *Cambeva stawiarski* (Miranda Ribeiro 1968). *J. Fish Biol.* **2021**, *96*, 350–363. [CrossRef]

20. Reis, V.J.C.; de Pinna, M.C.C. Diversity and systematics of *Trichomycterus* Valenciennes 1832 (Siluriformes: Trichomycteridae) in the Rio Doce Basin: Iterating DNA, phylogeny and classical taxonomy. *Zool. J. Linn. Soc.* **2022**. [CrossRef]

21. Katz, A.M.; Barbosa, M.A.; Mattos, J.L.O.; Costa, W.J.E.M. Multigene analysis of the catfish genus *Trichomycterus* and description of a new South American trichomycterine genus (Siluriformes, Trichomycteridae). *Zoosyst. Evol.* **2018**, *94*, 557–566. [CrossRef]

22. Gonçalves, C.d.S.; Carvalho, F.R.; Pérez-Mayorga, M.A.; Oliveira, I.F.d. Identification key for fishes from coastal streams of the Atlantic forest of southeastern Brazil. *Biota Neotropica* **2017**, *17*, e20170377. [CrossRef]

23. Bizerril, C.R.S.F. Descrição de uma nova espécie de *Trichomycterus* (Siluroidei, Trichomycteridae) do Estado de Santa Catarina, com a sinopse da composição da família Trichomycteridae no leste brasileiro. *Arq. Biol. Tecnol.* **1994**, *37*, 617–628.

24. Scarano, F.R.; Ceotto, P. Brazilian Atlantic forest: Impact, vulnerability, and adaptation to climate change. *Biodivers. Conserv.* **2015**, *24*, 2319–2331. [CrossRef]

25. Lopes, E.R.D.N.; Sales, J.C.A.; Sousa, J.A.P.D.; Amorim, A.T.; Albuquerque Filho, J.L.; Lourenço, R.W. Losses on the atlantic mata vegetation induced by land use changes. *Cerne* **2018**, *24*, 121–132. [CrossRef]

26. Myers, N.; Mittermeir, R.A.; Mittermeir, C.G.; da Fonseca, G.A.B.; Kent, J. Biodiversity hotspots for conservation priorities. *Nature* **2000**, *403*, 853–858. [CrossRef]

27. Carlucci, M.B.; Marcilio-Silva, V.; Torezan, J.M. The southern Atlantic Forest: Use, degradation, and perspectives for conservation. In *The Atlantic Forest: History, Biodiversity, Threats and Opportunities of the Mega-Diverse Forest*; Marques, M.C.M., Grelle, C.E.V., Eds.; Springer: Cham, Switzerland, 2021; pp. 91–111.

28. Oliveira, T.M.N.D.; Ribeiro, J.M.G.; Barros, V.G.; Simm, M.; Mello, Y.R.d.; Zeh, K.K. *Bacias Hidrográficas da Região de Joinville: Gestão e Dados*; Editora Univille: Joinville, Brazil, 2017.

29. Pinheiro, P.C.; Dalcin, R.H.; Batista, T.T. A ictiofauna de áreas com interesse para a proteção ambiental de Joinville, Santa Catarina, Brasil. *Acta Biol. Catarinense* **2017**, *4*, 73–89. [CrossRef]

30. Donin, L.M.; Ferrer, J.; Carvalho, T.P. Uncertainties and risks in delimiting species of *Cambeva* (Siluriformes: Trichomycteridae) with single-locus methods and geographically restricted data. *Neotrop. Ichthyol.* **2022**, *20*, e220019. [CrossRef]

31. Leary, S.; Underwood, W.; Anthony, R.; Cartner, S.; Corey, D.; Grandin, T.; Greenacre, C.; Gwaltney-Brant, S.; McCrackin, M.; Meyer, R.; et al. AVMA Guidelines for the Euthanasia of Animals: 2020 Edition. 2020. Available online: http://www.avma.org/sites/default/files/2020-02/Guidelines-on-Euthanasia-2020.pdf (accessed on 3 December 2022).

32. Taylor, W.R.; Van Dyke, G.C. Revised procedures for staining and clearing small fishes and other vertebrates for bone and cartilage study. *Cybium* **1985**, *9*, 107–119.

33. Costa, W.J.E.M. Description de huit nouvelles espèces du genre *Trichomycterus* (Siluriformes: Trichomycteridae), du Brésil oriental. *Rev. Française d'aquariologie et Herpetol.* **1992**, *18*, 101–110.

34. Costa, W.J.E.M.; Katz, A.M.; Mattos, J.L.O.; Amorim, P.F.; Mesquita, B.O.; Vilardo, P.J.; Barbosa, M.A. Historical review and redescription of three poorly known species of the catfish genus *Trichomycterus* from south-eastern Brazil (Siluriformes: Trichomycteridae). *J. Nat. Hist.* **2020**, *53*, 2905–2928. [CrossRef]

35. Bockmann, F.A.; Sazima, I. *Trichomycterus maracaya*, a new catfish from the upper rio Paraná, southeastern Brazil (Siluriformes: Trichomycteridae), with notes on the *T. brasiliensis* species-complex. *Neotrop. Ichthyol.* **2004**, *2*, 61–74. [CrossRef]

36. Arratia, G.; Huaquin, L. Morphology of the lateral line system and of the skin of diplomystic and certain primitive loricarioid catfishes and systematic and ecological considerations. *Bonn Zool. Monogr.* **1995**, *36*, 1–110.

37. De Queiroz, K. Species concepts and species delimitation. *Syst. Biol.* **2007**, *56*, 879–886. [CrossRef] [PubMed]

38. Davis, J.I.; Nixon, K.C. Populations, genetic variation, and the delimitation of phylogenetic species. *Syst. Biol.* **1992**, *41*, 421–435. [CrossRef]

39. Villa-Verde, L.; Lazzarotto, H.; Lima, S.Q.M. A new glanapterygine catfish of the genus *Listrura* (Siluriformes: Trichomycteridae) from southeastern Brazil, corroborated by morphological and molecular data. *Neotrop. Ichthyol.* **2012**, *10*, 527–538. [CrossRef]

40. Unmack, P.J.; Bennin, A.P.; Habi, E.M.; Victoriano, P.F.; Johnson, J.B. Impact of ocean barriers, topography, and glaciation on the phylogeography of the catfish *Trichomycterus areolatus* (Teleostei: Trichomycteridae) in Chile. *Biol. J. Linn. Soc.* **2009**, *97*, 876–892. [CrossRef]

41. Barros, L.C.; Santos, U.; Cioffi, M.D.B.; Dergam, J.A. Evolutionary divergence among *Oligosarcus* spp. Ostariophysi, Characidae from the São Francisco and Doce River Basins: Oligosarcus solitarius Menezes, 1987 shows the highest rates of chromosomal evolution in the Neotropical region. *Zebrafish* **2015**, *12*, 102–110. [CrossRef]

42. Ward, R.D.; Zemlak, T.S.; Innes, B.H.; Last, P.R.; Hebert, P.D. DNA barcoding Australia's fish species. Philos. *Trans. R. Soc. Lond. B Biol. Sci.* **2005**, *360*, 1847–1857. [CrossRef]

43. Hardman, M.; Page, L.M. Phylogenetic relationships among bullhead catfishes of the genus *Ameiurus* (Siluriformes: Ictaluridae). *Copeia* **2003**, *2003*, 20–33. [CrossRef]

44. Costa, W.J.E.M.; Henschel, E.; Katz, A.M. Multigene phylogeny reveals convergent evolution in small interstitial catfishes from the Amazon and Atlantic forests (Siluriformes: Trichomycteridae). *Zool. Scr.* **2020**, *49*, 159–173. [CrossRef]

45. Cramer, C.A.; Bonatto, S.L.; Reis, R.E. Molecular phylogeny of the Neoplecostominae and Hypoptopomatinae (Siluriformes: Loricariidae) using multiple genes. *Mol. Phylogenetics Evol.* **2011**, *59*, 43–52. [CrossRef] [PubMed]

46. Tamura, K.; Stecher, G.; Kumar, S. MEGA11: Molecular Evolutionary Genetics Analysis Version 11. *Mol. Biol. Evol.* **2021**, *38*, 3022–3027. [CrossRef] [PubMed]

47. Ochoa, L.E.; Roxo, F.F.; DoNascimiento, C.; Sabaj, M.H.; Datovo, A.; Alfaro, M.; Oliveira, C. Multilocus analysis of the catfish family Trichomycteridae (Teleostei: Ostariophysi: Siluriformes) supporting a monophyletic Trichomycterinae. *Mol. Phylogenet. Evol.* **2017**, *115*, 71–81. [CrossRef] [PubMed]

48. Chenna, R.; Sugawara, H.; Koike, T.; Lopez, R.; Gibson, T.J.; Higgins, D.G.; Thompson, J.D. Multiple sequence alignment with the Clustal series of programs. *Nucleic Acids Res.* **2003**, *31*, 3497–3500. [CrossRef]

49. Lanfear, R.; Frandsen, P.B.; Wright, A.M.; Senfeld, T.; Calcott, B. PartitionFinder 2: New methods for selecting partitioned models of evolution for molecular and morphological phylogenetic analyses. *Mol. Biol. Evol.* **2017**, *34*, 772–773. [CrossRef]

50. Ronquist, F.; Teslenko, M.; van der Mark, P.; Ayres, D.L.; Darling, A.; Höhna, S.; Larget, B.; Liu, L.; Suchard, M.A.; Huelsenbeck, J.P. MrBayes 3.2: Efficient Bayesian phylogenetic inference and model choice across a large model space. *Syst. Biol.* **2012**, *61*, 539–542. [CrossRef]

51. Rambaut, A.; Drummond, A.J.; Xie, D.; Baele, G.; Suchard, M.A. Posterior summarisation in Bayesian phylogenetics using Tracer 1.7. *Syst. Biol.* **2018**, *67*, 901–904. [CrossRef]

52. Nguyen, L.T.; Schmidt, H.A.; von Haeseler, A.; Minh, B.Q. IQ-TREE: A fast and effective stochastic algorithm for estimating maximum likelihood phylogenies. *Mol. Biol. Evol.* **2015**, *32*, 268–274. [CrossRef]

53. Minh, B.Q.; Nguyen, M.A.T.; von Haeseler, A. Ultrafast approximation for phylogenetic bootstrap. *Mol. Biol. Evol.* **2013**, *30*, 1188–1195. [CrossRef]

54. Felsenstein, J. Confidence limits on phylogenies: An approach using the bootstrap. *Evolution* **1985**, *39*, 783–791. [CrossRef]

55. Katz, A.M.; Barbosa, M.A. Re-description of *Trichomycterus cubataonis* Bizerril, 1994 (Siluriformes: Trichomycteridae) from the Cubatão river basin, southern Brazil. *Vertebrate Zool.* **2014**, *64*, 3–8.

56. de Pinna, M.C.C. A new subfamily of Trichomycteridae (Teleostei, Siluriformes), lower locarioid relationships and a discussion on the impact of additional taxa for phylogenetic analysis. *Zool. J. Linn. Soc.* **1992**, *106*, 175–229. [CrossRef]

57. Bockmann, F.A.; Casatti, L.; de Pinna, M.C.C. A new species of trichomycterid catfish from the Rio Paranapanema, southeastern Brazil (Teleostei; Siluriformes), with comments on the phylogeny of the family. *Ichthyol. Explor. Freshw.* **2004**, *15*, 225–242.

58. Wosiacki, W.B.; Garavello, J.C. Five new species of *Trichomycterus* from the Iguaçu (rio Paraná Basin), southern Brazil (Siluriformes: Trichomycteridae). *Ichthyol. Explor. Freshw.* **2004**, *15*, 1–16.

59. Ferrer, J.; Malabarba, L.R. Taxonomic review of the genus *Trichomycterus* Valenciennes (Siluriformes: Trichomycteridae) from the laguna dos Patos system, Southern Brazil. *Neotrop. Ichthyol.* **2013**, *11*, 217–246. [CrossRef]

60. Terán, G.E.; Ferrer, J.; Benitez, M.; Alonso, F.; Aguilera, G.; Mirande, J.M. Living in the waterfalls: A new species of *Trichomycterus* (Siluriformes: Trichomycteridae) from Tabay stream, Misiones, Argentina. *PLoS ONE* **2017**, *12*, e0179594. [CrossRef]

61. Zhang, J.; Kapli, P.; Pavlidis, P.; Stamatakis, A. A general species delimitation method with applications to phylogenetic placements. *Bioinformatics* **2013**, *29*, 2869–2876. [CrossRef]

62. Sukumaran, J.; Knowles, L.L. Multispecies coalescent delimits structure, not species. *Proc. Nat. Acad. Sci. USA* **2017**, *114*, 1607–1612. [CrossRef]

63. Pons, J.; Barraclough, T.G.; Gomez-Zurita, J.; Cardoso, A.; Duran, D.P.; Hazell, S.; Kamoun, S.; Sumlin, W.D.; Vogler, A.P. Sequence based species delimitation for the DNA taxonomy of undescribed insects. *Syst. Biol.* **2006**, *55*, 595–609. [CrossRef]

64. Fujisawa, T.; Barraclough, T.G. Delimiting species using single-locus data and the generalized mixed Yule coalescent approach: A revised method and evaluation on simulated data sets. *Syst. Biol.* **2013**, *62*, 707–724. [CrossRef]

65. Yu, G.; Rao, D.; Matsui, M.; Yang, J. Coalescent-based delimitation outperforms distance-based methods for delineating less divergent species: The case of *Kurixalus odontotarsus* species group. *Sci. Rep.* **2017**, *7*, 16124. [CrossRef] [PubMed]